Goal-oriented error estimation and adaptivity for free-boundary problems: the shape-linearization approach

SIAM J. SCI. COMPUT.
Vol. 32, No. 2, pp. 1093–1118

GOAL-ORIENTED ERROR ESTIMATION AND ADAPTIVITY FOR FREE-BOUNDARY PROBLEMS: THE SHAPE-LINEARIZATION APPROACH*

K. G. VAN DER ZEE†, E. H. VAN BRUMMELEN‡, AND R. DE BORST§

Abstract. We develop duality-based a posteriori error estimates for functional outputs of solutions of free-boundary problems via shape-linearization principles. To derive an appropriate dual (linearized adjoint) problem, we linearize the domain dependence of the very weak form and goal functional of interest using techniques from shape calculus. We show for a Bernoulli-type free-boundary problem that the dual problem corresponds to a Poisson problem with a Robin-type boundary condition involving the curvature. Moreover, we derive a generalization of the dual problem for nonsmooth free boundaries which includes a natural extension of the curvature term. The effectivity of the dual-based error estimate and its usefulness in goal-oriented adaptive mesh refinement is demonstrated by numerical experiments.

Key words. goal-oriented error estimation, a posteriori error estimation, Bernoulli free-boundary problem, shape derivative, shape differential calculus, linearized adjoint, adaptive mesh refinement

AMS subject classifications. 35R35, 49M29, 54C56, 58C20, 65N15, 65N50

DOI. 10.1137/080741239

1. Introduction.

This is the shape-linearization part of our work on goal-oriented error estimation and adaptivity for free-boundary problems; see also [42]. We consider duality-based a posteriori error estimates for functional outputs that include the dependence on both the error in the approximate solution and the error in the domain approximation.

In [42], we explained that free-boundary problems elude the standard goal-oriented error estimation framework because their typical variational form is noncanonical. In pursuit of a canonical form, we introduced the domain-map linearization approach at a reference domain which in essence reformulates the free-boundary problem to a fixed reference domain. Accordingly, the dual (linearized adjoint) problem is obtained by linearizing the transformed problem with respect to the domain map. This approach is straightforward. However, the dual problem contains nonstandard and nonlocal interior and boundary terms, which is inconvenient from an implementation point of view. Moreover, there is some arbitrariness in the dual problem due to the heuristic extension of boundary perturbations into the domain. A similar arbitrariness appears in shape optimization in the so-called material derivative approach [23, 36]. An elegant alternative in shape optimization is the shape derivative whose variational formulation consists only of standard interior and boundary terms.

*Received by the editors November 18, 2008; accepted for publication (in revised form) January 22, 2010; published electronically March 31, 2010.
http://www.siam.org/journals/sisc/32-2/74123.html

†Institute for Computational Engineering & Sciences (ICES), The University of Texas at Austin, 1 University Station C0200, Austin, TX 78712 (vanderzee@ices.utexas.edu). This work was done while the author was a Ph.D. student at the Delft University of Technology in The Netherlands.

‡Multiscale Engineering Fluid Dynamics (MEFD), Eindhoven University of Technology, PO Box 513, 5600 MB Eindhoven, The Netherlands (e.h.v.brummelen@tue.nl). This work was done while the author was employed at the Delft University of Technology in The Netherlands.

§Department of Mechanical Engineering, Eindhoven University of Technology, PO Box 513, 5600 MB Eindhoven, The Netherlands (r.d.borst@tue.nl).

Finding an analogous linearization approach for free-boundary problems has been the main motivation for this paper.

We present in this paper an approach to goal-oriented error estimation for free-boundary problems by shape-linearization principles. To illustrate the approach, we reconsider the Bernoulli-type free-boundary problem of [42]. We show that the associated very weak form and goal functional of interest can be formulated as a function of the unknown domain which can be linearized using techniques from shape calculus.

The shape-linearization approach does not pursue a canonical formulation and therefore requires a slight deviation from the standard goal-oriented error estimation framework, contrary to our approach in [42]. To obtain a suitable dual problem, the reasoning is as follows. The very weak form of the free-boundary problem and the goal functional of interest admit an appropriate shape linearization. This linearization yields a linear (adjoint) equation. In the standard goal-oriented error estimation framework, this linear equation directly defines the dual problem; see [1, 19, 33, 37]. In our case, however, the linear equation provides only a specification of the dual solution, but it does not suitably define the dual problem. Instead, we extract from the linear equation an appropriate dual problem by means of a consistent reformulation.

The dual problem can be found by straightforward variational arguments if the linearization takes place at a domain with a smooth free boundary. The dual problem then corresponds to a standard Poisson problem with a Robin boundary condition that involves the curvature. For nonsmooth free boundaries, however, the construction of an appropriate dual problem requires that we consider specific domain perturbations. This dual problem is a generalization of the smooth case that admits singular curvatures at singular points of the boundary.

It is noteworthy that many authors have presented linearizations of free-boundary problems in an effort to arrive at Newton-based iteration algorithms. Most of these address the free-boundary problem in a discretized setting; see, for instance, [10, 30, 38]. Our linearization is, however, in the continuous setting where one requires intricate shape differential calculus. It is therefore more related to Newton-based iteration algorithms in continuous settings as presented in [3, 16], for example. In particular, we mention the works of Kärkkäinen [26] and Kärkkäinen and Tiihonen [27, 28] who appropriately apply the techniques of shape differential calculus, though in a formal sense.

The contents of this paper are arranged as follows: Section 2 briefly presents the Bernoulli-type free-boundary model problem. In section 3, we review basic theory of shape differential calculus. In section 4, we apply shape linearization at smooth free boundaries to the very weak form of the free-boundary problem. Furthermore, we present the dual problem suitable for goal-oriented error estimation. Section 5 considers shape linearization at nonsmooth free boundaries. In section 6, we present numerical experiments and compare the shape-linearization approach with the domain-map linearization approach of [42]. Finally, section 7 contains concluding remarks.

2. Problem statement. We briefly present the Bernoulli-type free-boundary problem and a corresponding weak formulation, and we present several relevant goal functionals. In addition, we introduce a very weak form of the free-boundary problem which shall be suitable for shape linearization.

2.1. Bernoulli-type free-boundary problem. Let $D \subset \mathbb{R}^N$ denote a sufficiently large hold-all domain, and let $\mathcal{O}$ denote the set of bounded open Lipschitz domains $\Omega \subset D$, with boundary $\partial\Omega$ consisting of a fixed part $\Gamma_{\mathcal{D}}$ and a variable part Γ, referred to as the free boundary; see Figure 1. The Bernoulli-type free-boundary

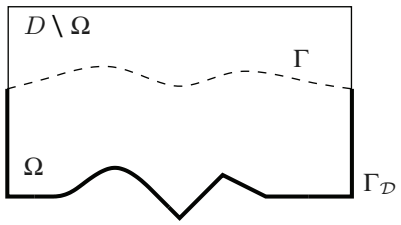

FIG. 1. *Geometric setup of the free-boundary problem: domain Ω, complement of Ω in the hold-all D (i.e., $D \setminus \Omega$), fixed boundary $\Gamma_{\mathcal{D}}$, and free boundary Γ.*

problem consists in seeking a domain $\Omega \in \mathcal{O}$ and a scalar function u defined on Ω such that

$$-\Delta u = f \qquad \text{in } \Omega\,, \tag{2.1a}$$

$$\partial_n u = g \qquad \text{on } \Gamma\,, \tag{2.1b}$$

$$u = h\big|_{\Gamma} = 1 \text{ on } \Gamma\,, \tag{2.1c}$$

$$u = h\big|_{\Gamma_{\mathcal{D}}} \qquad \text{on } \Gamma_{\mathcal{D}}\,, \tag{2.1d}$$

where we assume $f \in C^{0,1}(\overline{D})$ and $g \in C^{1,1}(\overline{D})$ together with a lower bound $g \geq g_0 > 0$ and $h \in C^{1,1}(\overline{D})$, with $C^{p,q}$ the (p,q) Hölder space. Note that, in accordance with (2.1c), $h|_\Gamma = 1$ is required for all admissible free boundaries. For general remarks concerning well posedness and numerical approximation of (2.1), we refer to our companion manuscript [42] and references therein. We assume the existence of a (possibly nonunique) domain $\Omega \subset \mathcal{O}$ and a corresponding solution $u \in H^1(\Omega)$ which solve (2.1).

Let $H^1_{0,\gamma}(\Omega)$ denote the space of H^1-functions with a zero trace on $\gamma \subseteq \partial\Omega$, i.e.,

$$H^1_{0,\gamma}(\Omega) := \left\{ v \in H^1(\Omega) :\ v = 0 \text{ on } \gamma \right\},$$

and let the (affine) space incorporating h be defined as $H^1_h(\Omega) := h|_\Omega + H^1_{0,\partial\Omega}(\Omega)$. A weak formulation of (2.1) is obtained by multiplying (2.1a) by $v \in H^1_{0,\Gamma_{\mathcal{D}}}(\Omega)$, integrating over Ω, and integrating by parts the Laplacian. As v is nonzero on Γ, we invoke (2.1b) to incorporate the Neumann boundary condition weakly. Furthermore, the Dirichlet boundary conditions (2.1c) and (2.1d) can be imposed strongly. We then arrive at the variational formulation:[1]

$$\boxed{\begin{array}{l}\text{Find } \Omega \in \mathcal{O} \text{ and } u \in H^1_h(\Omega) : \\ \qquad \displaystyle\int_\Omega \nabla u \cdot \nabla v = \int_\Omega f\, v + \int_\Gamma g\, v \qquad \forall v \in H^1_{0,\Gamma_{\mathcal{D}}}(\Omega)\,.\end{array}} \tag{2.2}$$

2.2. Errors in goal quantities. We are particularly interested in specific goal functionals of the solution $\mathcal{Q}(\Omega, u) \in \mathbb{R}$. In [42], we introduced two relevant goal functionals, viz., a weighted *average* of u and a weighted *elevation* of the free boundary,

$$\mathcal{Q}^{\text{ave}}(\Omega; u) := \int_\Omega q^{\text{ave}}\, u \qquad \text{and} \qquad \mathcal{Q}^{\text{elev}}(\Omega) := \int_{\Gamma_0} q^{\text{elev}}\, \alpha(\Omega)\,,$$

[1] For notational convenience we often neglect the integration measure in integrals. Domain and boundary integrals are to be integrated with respect to the usual volume and surface measures. For example, we write $\int_{\Gamma_\theta} f$ instead of $\int_{\Gamma_\theta} f \, \mathrm{d}\Gamma_\theta$.

respectively, where $q^{\text{ave}} \in H^1(D)$ and $q^{\text{elev}} \in L^2(\Gamma_0)$. The elevation $\alpha(\Omega) : \Gamma_0 \to \mathbb{R}$ is a scalar function which associates to a specific domain Ω the vertical deviation of the free boundary with respect to a horizontal rest position, Γ_0.

Given an approximate domain $\hat{\Omega} \in \mathcal{O}$ and corresponding approximation $u^{\mathsf{h}} \in H^1_h(\hat{\Omega})$, we aim at deriving by shape-linearization principles a dual-based estimate of the goal error

$$\mathcal{E}_{\mathcal{Q}} := \mathcal{Q}(\Omega, u) - \mathcal{Q}(\hat{\Omega}, u^{\mathsf{h}}) \, .$$

For this, the required dual problem is extracted from the linearization of the free-boundary problem and the goal functional with respect to (Ω, u). As usual, the linearization of the free-boundary problem yields the linearized adjoint operator, and the linearization of the goal functional yields the right-hand side for the dual problem.

2.3. Very weak form of the free-boundary problem. For a succesful linearization of the free-boundary problem, it is of crucial importance that we can vary Ω and u independent of each other for fixed test functions v. This is possible only if there are no Ω-dependent constraints on the u- and v-space. Furthermore, we need to view u and v as functions defined on the whole of D by suitably extending them outside Ω. This gives rise to the embedding $H^1(\Omega) \subset H^1(D) \; \forall \; \Omega \in \mathcal{O}$.

In view of the free-boundary constraint in the space $H^1_h(\Omega)$, the weak form in (2.2) is not suitable for the linearization. This constraint can be removed in two ways. The first is by means of a Lagrange multiplier that enforces the constraint $u = h$ on Γ. This is the approach taken by Kärkkäinen [26] and Kärkkäinen and Tiihonen [27, 28]. The downsides of this approach are the additional difficulty and dual interpretation of the Lagrange multiplier and the inability to perform the shape linearization without unnecessary smoothness assumptions. We therefore prefer a second approach, which enforces the constraint weakly. This approach does not encounter the above-mentioned problems.

A variational statement that weakly enforces Dirichlet boundary conditions is provided by the so-called very weak form. The function space that accommodates test functions for the very weak form is

$$H^1_{0,\Gamma_{\mathcal{D}}}(\Delta; D) := \left\{ v \in H^1_{0,\Gamma_{\mathcal{D}}}(D) : \, \Delta v \in L^2(D) \right\} .$$

The very weak form $\mathcal{N} : \big(\mathcal{O} \times H^1(D)\big) \times H^1_{0,\Gamma_{\mathcal{D}}}(\Delta; D) \to \mathbb{R}$ is given by

$$\mathcal{N}\big((\Omega, u); v\big) := \int_\Omega -u \, \Delta v - \int_\Omega f \, v - \int_\Gamma g \, v + \big\langle \partial_n v, h \big\rangle_{\partial\Omega} \, , \tag{2.3}$$

where the brackets, $\langle \cdot, \cdot \rangle_{\partial\Omega}$, imply a duality pairing of $H^{-1/2}(\partial\Omega)$ and $H^{1/2}(\partial\Omega)$. It can easily be verified that the free-boundary problem solutions $\Omega \in \mathcal{O}$ and $u \in H^1(\Omega) \subset H^1(D)$ satisfy

$$\mathcal{N}\big((\Omega, u); v\big) = 0 \qquad \forall v \in H^1_{0,\Gamma_{\mathcal{D}}}(\Delta; D) \, . \tag{2.4}$$

We are now ready to linearize $\mathcal{N}((\Omega, u); v)$ (for fixed v) and $\mathcal{Q}(\Omega, u)$ (viewing it as the map $\mathcal{Q} : \mathcal{O} \times H^1(D) \to \mathbb{R}$). The main difficulty in this linearization arises from the linearization with respect to Ω. This is dealt with by using techniques from shape differential calculus. The linearization can be performed under appropriate regularity requirements on the involved integrands. In the next section, we review these requirements and other essentials of shape calculus.

3. Shape differential calculus. In this section we give a brief summary of the theory of differential calculus of shape functionals. Most of the results presented in this section originate from early works in shape optimization by Simon [35], Pironneau [32], and Zolésio [43] and can be found in the books of Sokołowski and Zolésio [36] and Delfour and Zolésio [7]. Recent developments of shape derivatives under state constraints can be found in [24, 25], and shape derivatives for domains with cracks can be found, for instance, in [15, 17, 29].

A functional $\mathcal{J}$ is said to be a *shape functional* if it maps an admissible family $\mathcal{O}$ of domains into $\mathbb{R}$. Trivially then, for any homeomorphism T of $\overline{D}$ with $T(\Omega) = \Omega$,

$$\mathcal{J}(\Omega) = \mathcal{J}\big(T(\Omega)\big) \, .$$

A simple example is the volume integral given by $\mathcal{J}(\Omega) = \int_\Omega \mathrm{d}\Omega$. Note that for fixed $u \in H^1(D)$ and $v \in H^1_{0,\Gamma_\mathcal{D}}(\Delta; D)$, the maps $\Omega \mapsto \mathcal{N}\big((\Omega, u); v\big)$ and $\Omega \mapsto \mathcal{Q}(\Omega, u)$ are also shape functionals.

3.1. Definition of the shape derivative. Directional derivatives of $\mathcal{J}$ can be defined by considering one-parameter families of perturbed domains. Such a one-parameter family acts as a one-dimensional path along which limits of difference quotients can be taken. In this work, we construct families of perturbed domains by perturbations of the identity map $Id : \overline{D} \to \overline{D}$. Alternatively, they could have been constructed by means of the velocity method; see [7, 8] for results on the equivalence of both methods in the context of shape derivatives.

Let us denote by Θ the space of bounded Lipschitz perturbation-vector fields that vanish at $\Gamma_\mathcal{D}$, i.e.,

$$\Theta := \Big\{ \delta\theta \in C^{0,1}(\overline{D}; \mathbb{R}^N) : \, \delta\theta = 0 \text{ on } \Gamma_\mathcal{D} \Big\} \, .$$

For $\delta\theta \in \Theta$, we define the perturbed transformation map as $T_{\delta\theta} := Id + \delta\theta$, and for a given $\Omega \in \mathcal{O}$, the associated one-parameter family of domains and free boundaries is defined as

$$\Omega_t := T_{t\,\delta\theta}(\Omega) = \Big\{ x \in \mathbb{R}^N \big| \, x = T_{t\,\delta\theta}(X) \; \forall X \in \Omega \Big\} \, ,$$
$$\Gamma_t := T_{t\,\delta\theta}(\Gamma) = \Big\{ x \in \mathbb{R}^N \big| \, x = T_{t\,\delta\theta}(X) \; \forall X \in \Gamma \Big\} \, ,$$

respectively; see Figure 2. Note that $\Omega_0 = \Omega$. For small t, both $T_{t\,\delta\theta}$ and $T^{-1}_{t\,\delta\theta}$ are Lipschitz continuous and $\Omega_t \in \mathcal{O}$ [5, 7, 11]. Accordingly, the *Eulerian derivative* of the shape functional $\mathcal{J}$ at $\Omega \in \mathcal{O}$ in the direction $\delta\theta \in \Theta$ is defined as the following limit:

$$\boxed{\mathcal{J}'(\Omega)(\delta\theta) := \lim_{t \to 0} \frac{\mathcal{J}(\Omega_t) - \mathcal{J}(\Omega)}{t} \, .}$$

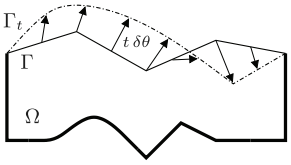

FIG. 2. *A perturbation of Ω by $t\,\delta\theta$ generates the domain Ω_t with free boundary Γ_t.*

We refer to this derivative as the *shape derivative* of $\mathcal{J}$. Note that the shape derivative coincides with the Gâteaux derivative of the map $\theta \mapsto \mathcal{J}(T_\theta(\Omega))$ at $\theta = 0$ in the direction $\delta\theta$; see [8, 11, 31] for Gâteaux derivative approaches. A useful consequence of the definition of the shape derivative is Taylor series identities such as

$$\begin{aligned} \mathcal{J}(\Omega_1) &= \mathcal{J}(\Omega_0) + \int_0^1 \mathcal{J}'(\Omega_t)(\delta\theta)\,\mathrm{d}t \\ &= \mathcal{J}(\Omega_0) + \mathcal{J}'(\Omega_0)(\delta\theta) + o(\|\delta\theta\|)\,. \end{aligned} \tag{3.1}$$

The shape functional $\mathcal{J}$ is said to be *shape differentiable* at Ω with respect to Θ if the shape derivative $\mathcal{J}'(\Omega)(\delta\theta)$ exists in all directions $\delta\theta \in \Theta$ and, moreover, the map $\delta\theta \mapsto \mathcal{J}'(\Omega)(\delta\theta)$ is linear and continuous on Θ. The functional $\mathcal{J}'(\Omega)$ is called the *shape gradient* of $\mathcal{J}$ (at Ω).

3.2. Structure of the shape derivative. It is expected that $\mathcal{J}'(\Omega)(\delta\theta)$ is nonzero only if $\delta\theta$ is nonzero at the boundary Γ. This is made precise in the following theorem. Its proof can be found in [5, 7, 36].

THEOREM 3.1 (Hadamard-Zolésio structure theorem). *If $\mathcal{J}$ is shape differentiable at Ω with respect to Θ, then its shape gradient $\mathcal{J}'(\Omega)$ is supported (as a distribution) on Γ. Furthermore, if Γ is sufficiently smooth (dependent on Θ[2]), then there exists a scalar Γ-distribution $j'(\Gamma)$ such that*

$$\boxed{\mathcal{J}'(\Omega)(\delta\theta) = \big\langle j'(\Gamma), \gamma(\delta\theta)\cdot n\big\rangle_\Gamma\,,} \tag{3.2}$$

where $\gamma(\cdot)$ is the trace operator on Γ.

Indeed, the first part of the theorem states that the shape derivative only depends on $\delta\theta$ at Γ. Moreover, if Γ is smooth enough, then it depends only on the normal component $\delta\theta \cdot n$. In particular, if $j'(\Gamma) \in L^1(\Gamma)$, then (3.2) can be written as

$$\mathcal{J}'(\Omega)(\delta\theta) = \int_\Gamma j'(\Gamma)\,\delta\theta\cdot n\,. \tag{3.2$*$}$$

Although Hadamard [21] derived (3.2$*$) in 1907 for boundary normal-perturbations of a C^∞-domain, it is generally known as the *Hadamard formula*. Furthermore, in his pioneering book [32], Pironneau's definition of Γ-*differentiability* of a shape functional $\mathcal{J}$ presumes precisely the existence of $j'(\Gamma) \in L^1(\Gamma)$ under the stronger notion of the Fréchet differentiability of $\theta \mapsto \mathcal{J}(T_\theta(\Omega))$.

In the following sections, we derive the shape derivative of the two most common shape functionals: a domain integral and a boundary integral.

3.3. Shape derivative of a domain integral. Consider the shape functional $\mathcal{J} : \mathcal{O} \to \mathbb{R}$ defined as the domain integral of a global function $\phi \in W^{1,1}(D)$, where $W^{m,p}(D)$ is the (m,p)-Sobolev space on D,

$$\mathcal{J}(\Omega) = \int_\Omega \phi\,\mathrm{d}x\,. \tag{3.3}$$

To compute the shape derivative in the direction $\delta\theta \in \Theta$, note that $\mathcal{J}(\Omega_t)$ can be written as an integral over Ω:

$$\mathcal{J}(\Omega_t) = \int_{\Omega_t} \phi\,\mathrm{d}x = \int_\Omega (\phi \circ T_{t\,\delta\theta})\,|J_t|\,\mathrm{d}x\,,$$

[2] Assume Γ of class C^{k+1} if $\Theta \subset C^k(\overline{D}, \mathbb{R}^N)$.

where $J_t := \det \mathrm{D}T_{t\,\delta\theta}$ is the Jacobian of $T_{t\,\delta\theta}$, with $\mathrm{D}(\cdot) := \partial(\cdot)/\partial(x_1, \ldots, x_N)$ the Jacobian matrix. We have $J_t \in L^\infty(D)$ (by Rademacher's theorem [14, p. 91]), $J_t > 0$ for small t, and

$$\frac{\partial}{\partial t} J_t\big|_{t=0} = \operatorname{div} \delta\theta \in L^\infty(D) \; ;$$

see [7, p. 352], for example. Furthermore, the derivative of $t \mapsto \phi \circ T_{t\,\delta\theta}$ is given by

$$\frac{\partial}{\partial t}(\phi \circ T_{t\,\delta\theta})\big|_{t=0} = \nabla\phi \cdot \delta\theta \in L^1(\Omega) \; . \tag{3.4}$$

With these results, we have the following [7, 36] proposition.

PROPOSITION 3.2 (shape derivative of domain integral). *For $\phi \in W^{1,1}(D)$, the shape functional in* (3.3) *is shape differentiable at $\Omega \in \mathcal{O}$ with respect to Θ. The shape derivative is given by*

$$\boxed{\mathcal{J}'(\Omega)(\delta\theta) = \int_\Omega \operatorname{div}\left(\phi\, \delta\theta\right) = \int_\Gamma \phi\, \delta\theta \cdot n \; .}$$

In view of the structure theorem, Theorem 3.1, it is clear that the scalar distribution $j'(\Gamma)$ associated with the shape gradient $\mathcal{J}'(\Omega)$ is equal to $\gamma(\phi) \in L^1(\Gamma)$.

It is clear from Proposition 3.2 that the shape derivative vanishes if $\phi = 0$ at Γ. This holds also for less regular ϕ corresponding to the product of two functions of which one vanishes at Γ.

PROPOSITION 3.3. *Let $\phi = \phi_1\, \phi_2$, where $\phi_1 \in L^2(D)$ and $\phi_2 \in H^1(D)$ with $\phi_2 = 0$ on Γ. Then the shape functional in* (3.3) *is shape differentiable at $\Omega \in \mathcal{O}$ with respect to Θ, and its shape derivative vanishes:*

$$\mathcal{J}'(\Omega)(\delta\theta) = 0 \; .$$

As it appears that this result is new, we give the proof in Appendix B.

3.4. Shape derivative of a boundary integral. Consider the shape functional $\mathcal{J} : \mathcal{O} \to \mathbb{R}$ defined as the boundary integral of a global function $\psi \in W^{2,1}(D)$:

$$\mathcal{J}(\Omega) = \int_\Gamma \psi \; \mathrm{d}\Gamma \; . \tag{3.5}$$

To obtain the shape derivative for perturbation $\delta\theta \in \Theta$, rewrite $\mathcal{J}(\Omega_t)$ as a boundary integral at Γ,

$$\mathcal{J}(\Omega_t) = \int_{\Gamma_t} \psi = \int_\Gamma (\psi \circ T_{t\,\delta\theta})\, \omega_t \; \mathrm{d}\Gamma \; ,$$

where $\omega_t := J_t \big| \mathrm{D}T_{t\,\delta\theta}^{-\mathsf{T}} \cdot n \big| : \Gamma \to \mathbb{R}$ is a surface density, referred to as the tangential Jacobian [11]. We have $\omega_t \in L^\infty(\Gamma)$ for small t and

$$\frac{\partial}{\partial t} \omega_t\big|_{t=0} = \operatorname{div}_\Gamma \delta\theta \in L^\infty(\Gamma) \; ;$$

see [36, p. 80], for example. The tangential (or surface) divergence is defined as $\operatorname{div}_\Gamma(\cdot) = \operatorname{div}(\cdot)\big|_\Gamma - \mathrm{D}(\cdot)\, n \cdot n = \operatorname{div}(\cdot)\big|_\Gamma - \partial_n(\cdot) \cdot n$. To differentiate $\psi \circ T_{t\,\delta\theta}$, we

apply (3.4) and note that at Γ a gradient splits up into a tangential (or surface) gradient and a normal component, i.e., $\nabla(\cdot) = \nabla_\Gamma(\cdot) + \partial_n(\cdot)\, n$. Hence, we have

$$\frac{\partial}{\partial t}(\psi \circ T_{t\,\delta\theta})\big|_{t=0} = \partial_n\psi\, \delta\theta \cdot n + \nabla_\Gamma\psi \cdot \delta\theta \in L^1(\Gamma)\ .$$

We refer to [6–9] for further remarks concerning tangential calculus. The shape derivative of $\mathcal{J}$ readily follows from these results.

PROPOSITION 3.4 (shape derivative of boundary integral). *For $\psi \in W^{2,1}(D)$, the shape functional in* (3.5) *is shape differentiable at Ω with respect to Θ. The shape derivative is given by*

$$\boxed{\mathcal{J}'(\Omega)(\delta\theta) = \int_\Gamma \Big(\partial_n\psi\, \delta\theta \cdot n + \nabla_\Gamma\psi \cdot \delta\theta + \psi\ \mathrm{div}_\Gamma\, \delta\theta\Big)\ .}$$

In accordance with the structure theorem, Theorem 3.1, the shape gradient of $\mathcal{J}$ is supported on Γ. However, as Ω is assumed to be Lipschitz, the boundary Γ is generally not smooth enough for the Hadamard formula (3.2$*$) to hold. Indeed, if Γ is assumed to be $C^{1,1}$, we can apply the following tangential Green's identity (see [36, p. 86] or [7, 9], for example):

$$\int_\Gamma \big(\psi\ \mathrm{div}_\Gamma\, \delta\theta + \nabla_\Gamma\psi \cdot \delta\theta\big) = \int_\Gamma \kappa\, \psi\, \delta\theta \cdot n\ ,$$

where $\kappa := \mathrm{div}_\Gamma\, n \in L^\infty(\Gamma)$ coincides with the additive curvature (sum of $N-1$ curvatures) of Γ. Accordingly, the shape derivative can be simplified to

$$\mathcal{J}'(\Omega)(\delta\theta) = \int_\Gamma \big(\partial_n\psi + \kappa\, \psi\big)\ \delta\theta \cdot n\ \mathrm{d}\Gamma\ . \tag{3.6}$$

Hence, $j'(\Gamma)$ in (3.2$*$) can be identified with $\partial_n\psi + \kappa\,\psi \in L^1(\Gamma)$.

The regularity requirement $\psi \in W^{2,1}(D)$ implying $j'(\Gamma) \in L^1(\Gamma)$ in (3.6) can be weakened for our purposes by considering it as a member of the space

$$H^1(\Delta; D) := \Big\{\psi \in H^1(D) : \Delta\psi \in L^2(D)\Big\}\ .$$

We can then extend (3.6) to hold $\forall\ \psi \in H^1(\Delta; D)$, provided we interpret the integral as a duality pairing and view the normal derivative as a member of a suitable dual space, i.e., $[H^{1/2}_{00}(\Gamma)]'$. We shall denote the derivative in this case by

$$\mathcal{J}'(\Omega)(\delta\theta) = \big\langle \partial_n\psi\ ,\ \delta\theta \cdot n\big\rangle_\Gamma + \int_\Gamma \kappa\, \psi\, \delta\theta \cdot n\ .$$

4. Goal-oriented error estimation by shape linearization at smooth free boundaries. We now turn our attention to goal-oriented error estimation for the free-boundary problem (2.1). We proceed by linearizing the very weak form and the goal functional at the approximation $(\hat\Omega, u^{\mathsf{h}}) \in \mathcal{O} \times H^1_{\hat h}(\hat\Omega)$. In this section, we assume that the approximate free boundary $\hat\Gamma$ is sufficiently smooth; i.e., $\hat\Gamma$ is a $C^{1,1}$ boundary. The more general case of Lipschitz continuous free boundaries is taken up in section 5.

4.1. Linearization of the free-boundary problem. We can write the very weak form given in (2.3) as

$$\mathcal{N}\big((\Omega,u);v)\big) = -\mathcal{B}(\Omega;u,v) - \mathcal{F}(\Omega;v) - \mathcal{G}(\Omega;v) + \mathcal{H}(\Omega;v)\ , \tag{4.1}$$

where the semilinear forms are defined as

$$\mathcal{B}(\Omega;u,v) := \int_\Omega u\,\Delta v\ , \qquad \mathcal{F}(\Omega;v) := \int_\Omega f\,v\ ,$$
$$\mathcal{H}(\Omega;v) := \int_\Omega \big(h\,\Delta v + \nabla h\cdot\nabla v\big)\ , \qquad \mathcal{G}(\Omega;v) := \int_\Gamma g\,v\ .$$

Note that we replaced the duality pairing $\langle \partial_n v, h\rangle_{\partial\Omega}$ with two domain integrals; this shall be convenient for the shape derivative.

Consider a fixed $v \in H^1_{0,\Gamma_\mathcal{D}}(\Delta;D)$. The linearization of $u \mapsto \mathcal{N}((\hat\Omega,u);v)$ at $u^\mathsf{h} \in H^1_h(\hat\Omega) \subset H^1(D)$ is straightforward as only $\mathcal{B}$ depends on u, and moreover, this dependence is linear. Denoting this derivative by $\langle \partial_u(\cdot), \delta u\rangle$, we have

$$\boxed{\big\langle \partial_u \mathcal{N}\big((\hat\Omega,u^\mathsf{h});v\big), \delta u\big\rangle = \int_{\hat\Omega} -\delta u\,\Delta v} \tag{4.2a}$$

$\forall\ \delta u \in H^1_{0,\Gamma_\mathcal{D}}(D)$. This implies that the linearized adjoint operator corresponds to the negative Laplacian in $\hat\Omega$.

The shape linearization of $\Omega \mapsto \mathcal{N}((\Omega,u^\mathsf{h});v)$ at $\hat\Omega$ splits up into three contributions, each following from results of section 3. As the first contribution, we consider the combined $\mathcal{B}$- and $\mathcal{H}$-term:

$$-\mathcal{B}(\Omega;u^\mathsf{h},v) + \mathcal{H}(\Omega;v) = \int_\Omega -(u^\mathsf{h}-h)\,\Delta v + \int_\Omega \nabla h\cdot\nabla v\ .$$

Observe that $(u^\mathsf{h}-h)$ and ∇h are in $H^1(D)$ and vanish on $\hat\Gamma$ on account of $u^\mathsf{h} \in H^1_h(\hat\Omega)$ and $h = 1$ on all admissible free boundaries. Hence, by Proposition 3.3, the shape derivatives of these terms are zero. To obtain the shape derivative of $\mathcal{F}(\Omega;v)$, we can invoke Proposition 3.2 since $fv \in W^{1,1}(D)$. For $\delta\theta \in \Theta$, this gives

$$\mathcal{F}'(\hat\Omega;v)(\delta\theta) = \int_{\hat\Gamma} f\,v\,\delta\theta\cdot n\ .$$

For the final contribution, $\mathcal{G}(\Omega;v)$, we note that $g \in C^{0,1}(\overline{D})$ and $v \in H^1_{0,\Gamma_\mathcal{D}}(\Delta;D)$. Furthermore, since $\hat\Gamma$ is $C^{1,1}$, we can use a weak version of (3.6), yielding

$$\mathcal{G}'(\hat\Omega;v)(\delta\theta) = \big\langle g\,\partial_n v\ ,\ \delta\theta\cdot n\big\rangle_{\hat\Gamma} + \int_{\hat\Gamma} (\partial_n g + \kappa\, g)\,v\,\delta\theta\cdot n\ .$$

We summarize these results in the following proposition.

PROPOSITION 4.1 (shape derivative of free-boundary problem: smooth $\hat\Gamma$). *Let $\hat\Omega \in \mathcal{O}$ with $C^{1,1}$ free boundary $\hat\Gamma$. For any $u^\mathsf{h} \in H^1_h(\hat\Omega) \subset H^1(D)$ and $v \in H^1_{0,\Gamma_\mathcal{D}}(\Delta;D)$, the shape functional $\Omega \mapsto \mathcal{N}((\Omega,u^\mathsf{h});v)$ is shape differentiable at $\hat\Omega$ with respect to Θ. Its shape derivative is given by*

$$\boxed{\big\langle \partial_\Omega \mathcal{N}\big((\hat\Omega,u^\mathsf{h});v\big), \delta\theta\big\rangle = -\big\langle g\,\partial_n v\ ,\ \delta\theta\cdot n\big\rangle_{\hat\Gamma} - \int_{\hat\Gamma} \big(f + \partial_n g + \kappa\, g\big)\,v\,\delta\theta\cdot n\ .} \tag{4.2b}$$

From this proposition it is clear that the shape gradient can be identified with the boundary distribution

$$j'(\hat{\Gamma}) = -g\,\partial_n v - (f + \partial_n g + \kappa\, g)\, v\ .$$

Essentially, this implies that the linearized adjoint operator corresponds to a Robin-type boundary condition on $\hat{\Gamma}$.

4.2. Linearization of the goal functional. We consider the goal functional consisting of a linear combination of the average and elevation functional; see section 2.2:

$$\mathcal{Q}(\Omega, u) = \mathcal{Q}^{\text{ave}}(\Omega; u) + \mathcal{Q}^{\text{elev}}(\Omega) = \int_\Omega q^{\text{ave}}\, u + \int_{\Gamma_0} q^{\text{elev}}\, \alpha(\Omega).$$

Again, the linearization with respect to u is straightforward,

$$\boxed{\left\langle \partial_u \mathcal{Q}(\hat{\Omega}, u^{\mathsf{h}}), \delta u \right\rangle = \int_{\hat{\Omega}} q^{\text{ave}}\, \delta u} \tag{4.3a}$$

$\forall\ \delta u \in H^1_{0,\Gamma_{\mathcal{D}}}(D)$. The shape linearization of $\Omega \mapsto \mathcal{Q}^{\text{ave}}(\Omega; u^{\mathsf{h}})$ follows from Proposition 3.2 as $q^{\text{ave}} u^{\mathsf{h}} \in W^{1,1}(D)$ for $q^{\text{ave}}, u \in H^1(D)$. Furthermore, the shape linearization of $\Omega \mapsto \mathcal{Q}^{\text{elev}}(\Omega; u^{\mathsf{h}})$ was given in the appendix of [42], where we employed a Gâteaux derivative approach for the elevation function $\theta \mapsto \alpha(T_\theta(\Omega))$. Combining these results, we have for $\delta\theta \in \Theta$ that

$$\boxed{\left\langle \partial_\Omega \mathcal{Q}(\hat{\Omega}, u^{\mathsf{h}}), \delta\theta \right\rangle = \int_{\hat{\Gamma}} \left(q^{\text{ave}} + q^{\text{elev}}\right) \delta\theta \cdot n\ .} \tag{4.3b}$$

Note that we substituted $u^{\mathsf{h}} = h = 1$ on $\hat{\Gamma}$. Furthermore, since q^{elev} is only defined on a horizontal rest position Γ_0, it should be interpreted with the aid of a projection along the x_N-axis, that is,

$$q^{\text{elev}}(x_1, \ldots, x_N) = q^{\text{elev}}(x_1, \ldots, x_{N-1}, x_N^{\Gamma_0}),$$

with $x_N^{\Gamma_0}$ being the x_N-coordinate of Γ_0. The result in (4.3b) is valid for any $\hat{\Omega} \in \mathcal{O}$; i.e., a $C^{1,1}$ free boundary is not required.

4.3. Dual problem and goal-error estimate. We are now ready to define the appropriate dual problem based on the linearized adjoint operator and goal functional linearization. Let the dual solution z be defined as the solution of the following variational problem:

$$\boxed{\begin{aligned} &\text{Find } z \in H^1_{0,\Gamma_{\mathcal{D}}}(\hat{\Omega}) : \\ &\qquad \int_{\hat{\Omega}} \nabla\delta u \cdot \nabla z + \int_{\hat{\Gamma}} \tfrac{1}{g}(f + \partial_n g + \kappa\, g)\, z\, \delta u \\ &\qquad\quad = \int_{\hat{\Omega}} q^{\text{ave}}\, \delta u - \int_{\hat{\Gamma}} \tfrac{1}{g}(q^{\text{ave}} + q^{\text{elev}})\, \delta u \qquad \forall \delta u \in H^1_{0,\Gamma_{\mathcal{D}}}(\hat{\Omega})\ . \end{aligned}} \tag{4.4}$$

It can easily be shown that z is a weak solution of the following Poisson problem with a Robin-type boundary condition at the approximate free boundary $\hat{\Gamma}$:

$$-\Delta z = q^{\text{ave}} \qquad \text{in } \hat{\Omega}\ , \tag{4.5a}$$

$$g\,\partial_n z + (f + \partial_n g + \kappa\, g)\, z = -(q^{\text{elev}} + q^{\text{ave}}) \quad \text{on } \hat{\Gamma}\ , \tag{4.5b}$$

$$z = 0 \qquad \text{on } \Gamma_{\mathcal{D}}\ . \tag{4.5c}$$

Note that on account of coercivity, a unique solution of (4.4) exists if $(f+\partial_n g)/g+\kappa \geq 0$. Under the implied requirements of the data, we obtain from (4.5a) and (4.5c) that $z \in H^1_{0,\Gamma_{\mathcal{D}}}(\Delta; D)$ and from (4.5b) that $\partial_n z \in L^2(\hat{\Gamma})$. We remark that similar conditions on the data are given in [12, 13] in a completely different setting of the Bernoulli free-boundary problem, though.

The main result of this section is that this dual problem provides a solution that is consistent with the linearization. We outline this in the following theorem, whose proof is delayed until the end of this section.

THEOREM 4.2 (dual consistency: smooth $\hat{\Gamma}$). *Given an approximation $(\hat{\Omega}, u^{\mathsf{h}}) \in \mathcal{O} \times H^1_h(\hat{\Omega})$, with a $C^{1,1}$ free boundary $\hat{\Gamma}$, of the solution $(\Omega, u) \in \mathcal{O} \times H^1_h(\Omega)$ of the free-boundary problem* (2.1)*, the solution $z \in H^1_{0,\Gamma_{\mathcal{D}}}(\hat{\Omega}) \subset H^1(D)$ of dual problem* (4.4) *satisfies*

$$\mathcal{N}'\big((\hat{\Omega}, u^{\mathsf{h}}); z\big)(\delta\theta, \delta u) = \mathcal{Q}'\big(\hat{\Omega}, u^{\mathsf{h}}\big)(\delta\theta, \delta u)$$

$\forall\ (\delta\theta, \delta u) \in \Theta \times H^1_{0,\Gamma_{\mathcal{D}}}(D)$.

If we compare the shape-linearized dual problem (4.4) with the dual problem obtained by domain-map linearization in [42], we notice that the dual problem in [42] contains a nonlocal residual-type boundary term. However, at the free-boundary problem solution (Ω, u), this residual-type term vanishes, and both dual problems are equivalent.

From the standard goal-oriented error estimation framework, it is clear that dual consistency plays a key role in goal-oriented error estimates; see section 3 of [42]. To present this estimate, let $e_\Omega \in \Theta$ denote a nontrivial perturbation-vector field such that $\Omega = T_{e_\Omega}(\hat{\Omega})$. Then $\|e_\Omega\|$ essentially measures the domain difference between Ω and $\hat{\Omega}$. Let e_u denote the error in u by subtracting u^{h} from it, thereby viewing u and u^{h} as members of $H^1(D)$. Since both $u = h$ and $u^{\mathsf{h}} = h$ on $\Gamma_{\mathcal{D}}$, we have $e_u := u - u^{\mathsf{h}} \in H^1_{0,\Gamma_{\mathcal{D}}}(D)$. The following proposition shows that, up to high-order terms, the error in our goal is related to the residual at $(\hat{\Omega}, u^{\mathsf{h}})$:

$$v \mapsto \mathcal{R}\big((\hat{\Omega}, u^{\mathsf{h}}); v\big) := \int_{\hat{\Omega}} f\, v + \int_{\hat{\Gamma}} g\, v - \int_{\hat{\Omega}} \nabla u^{\mathsf{h}} \cdot \nabla v\ .$$

PROPOSITION 4.3 (goal-error estimate: smooth $\hat{\Gamma}$). *Under the conditions of Theorem* 4.2*, let $z \in H^1_{0,\Gamma_{\mathcal{D}}}(\hat{\Omega})$ be the solution of dual problem* (4.4)*. It holds that*

$$\boxed{\mathcal{E}_{\mathcal{Q}} := \mathcal{Q}(\Omega, u) - \mathcal{Q}(\hat{\Omega}, u^{\mathsf{h}}) = \mathcal{R}\big((\hat{\Omega}, u^{\mathsf{h}}); z\big) + R\ ,} \tag{4.6}$$

where the remainder R is $o(\|e_\Omega\|, \|e_u\|)$.

Proof. The proof follows closely the proof of Theorem 3.1 in [42]. We first derive the following Taylor series expressions. Applying (3.1) to $\Omega \mapsto \mathcal{Q}(\Omega, u^{\mathsf{h}})$, we have

$$\mathcal{Q}(\Omega, u^{\mathsf{h}}) = \mathcal{Q}(\hat{\Omega}, u^{\mathsf{h}}) + \big\langle \partial_\Omega \mathcal{Q}(\hat{\Omega}, u^{\mathsf{h}})\ ,\ e_\Omega \big\rangle + o(\|e_\Omega\|)\ .$$

For the linearization of $\mathcal{Q}$ with respect to both its arguments, this implies the Taylor series formula

$$\mathcal{Q}(\Omega, u) = \mathcal{Q}(\hat{\Omega}, u^{\mathsf{h}}) + \mathcal{Q}'(\hat{\Omega}, u^{\mathsf{h}})(e_\Omega, e_u) + o(\|e_\Omega\|, \|e_u\|)\ . \tag{4.7}$$

We have a similar expression for $\mathcal{N}$:

$$\mathcal{N}\big((\Omega, u); v\big) = \mathcal{N}\big((\hat{\Omega}, u^{\mathsf{h}}); v\big) + \mathcal{N}'\big((\hat{\Omega}, u^{\mathsf{h}}); v\big)(e_\Omega, e_u) + o(\|e_\Omega\|, \|e_u\|) \tag{4.8}$$

for any $v \in H^1_{0,\Gamma_\mathcal{D}}(\Delta; D)$. Consider the goal error $\mathcal{E}_\mathcal{Q} = \mathcal{Q}(\Omega, u) - \mathcal{Q}(\hat{\Omega}, u^\mathsf{h})$. Using the Taylor series formula (4.7) and the dual-consistency theorem, Theorem 4.2, we obtain

$$\mathcal{E}_\mathcal{Q} = \mathcal{Q}'(\hat{\Omega}, u^\mathsf{h})(e_\Omega, e_u) + o(\|e_\Omega\|, \|e_u\|) = \mathcal{N}'\big((\hat{\Omega}, u^\mathsf{h}); z\big)(e_\Omega, e_u) + o(\|e_\Omega\|, \|e_u\|) \; .$$

Since $z \in H^1_{0,\Gamma_\mathcal{D}}(\Delta; D)$, we can invoke (4.8) to obtain

$$\mathcal{E}_\mathcal{Q} = \mathcal{N}\big((\Omega, u); z\big) - \mathcal{N}\big((\hat{\Omega}, u^\mathsf{h}); z\big) + o(\|e_\Omega\|, \|e_u\|) \; .$$

The first term on the right-hand side vanishes on account of consistency of the solution (Ω, u) with the very weak form; see (2.4). Furthermore, expanding $\mathcal{N}((\hat{\Omega}, u^\mathsf{h}); z)$ in accordance with (2.3), it follows that

$$\mathcal{E}_\mathcal{Q} = \int_{\hat{\Omega}} u^\mathsf{h} \, \Delta z + \int_{\hat{\Omega}} f \, z + \int_{\hat{\Gamma}} g \, z - \big\langle \partial_n z, h \big\rangle_{\partial\hat{\Omega}} + o(\|e_\Omega\|, \|e_u\|) \; .$$

Finally, by applying an integration by parts on the first term and using $u^\mathsf{h} = h$ on $\partial\hat{\Omega}$, we obtain the proof. ∎

Proof of Theorem 4.2. The linear equation in Theorem 4.2 can be logically separated into two equations corresponding to δu and $\delta\theta$:

$$\big\langle \partial_u \mathcal{N}\big((\hat{\Omega}, u^\mathsf{h}); z\big), \delta u \big\rangle = \big\langle \partial_u \mathcal{Q}(\hat{\Omega}, u^\mathsf{h}), \delta u \big\rangle \qquad \forall \delta u \in H^1_{0,\Gamma_\mathcal{D}}(D) \; , \tag{4.9a}$$

$$\big\langle \partial_\Omega \mathcal{N}\big((\hat{\Omega}, u^\mathsf{h}); z\big), \delta\theta \big\rangle = \big\langle \partial_\Omega \mathcal{Q}(\hat{\Omega}, u^\mathsf{h}), \delta\theta \big\rangle \qquad \forall \delta\theta \in \Theta \; . \tag{4.9b}$$

First, we show that z satisfies (4.9a). The explicit expression of (4.9a) follows from (4.2a) and (4.3a) and is given by

$$\int_{\hat{\Omega}} -\delta u \, \Delta z = \int_{\hat{\Omega}} q^{\text{ave}} \, \delta u \qquad \forall \delta u \in H^1_{0,\Gamma_\mathcal{D}}(D) \; .$$

Since $H^1_{0,\Gamma_\mathcal{D}}(\hat{\Omega})$ is dense in $L^2(\hat{\Omega})$, we essentially need to show that

$$-\Delta z = q^{\text{ave}} \quad \text{a.e. in } \hat{\Omega} \; . \tag{4.10}$$

This follows from (4.4) by elementary variational arguments: Choosing a δu in (4.4) that vanishes on $\partial\hat{\Omega}$, i.e., $\delta u \in H^1_{0,\partial\hat{\Omega}}(\hat{\Omega})$, we have

$$\int_{\hat{\Omega}} \nabla \delta u \cdot \nabla z = \int_{\hat{\Omega}} q^{\text{ave}} \, \delta u \; ,$$

and an integration by parts on the left-hand side followed by a density argument proves (4.10). We next show that z satisfies (4.9b). An explicit expression of (4.9b) follows from (4.2b) and (4.3b). Hence, we need to show that

$$-\big\langle g \, \partial_n z \, , \, \delta\theta \cdot n \big\rangle_{\hat{\Gamma}} - \int_{\hat{\Gamma}} \big(f + \partial_n g + \kappa \, g\big) \, z \, \delta\theta \cdot n = \int_{\hat{\Gamma}} \big(q^{\text{ave}} + q^{\text{elev}}\big) \, \delta\theta \cdot n \tag{4.11}$$

$\forall \; \delta\theta \in \Theta$. For this, we integrate by parts the first integral in (4.4) and use the fact that z satisfies (4.10) to obtain

$$\big\langle \partial_n z, \delta u \big\rangle_{\hat{\Gamma}} + \int_{\hat{\Gamma}} \frac{1}{g} (f + \partial_n g + \kappa \, g) \, z \, \delta u = - \int_{\hat{\Gamma}} \frac{1}{g} (q^{\text{ave}} + q^{\text{elev}}) \, \delta u$$

$\forall \; \delta u \in H^1_{0,\Gamma_\mathcal{D}}(\hat{\Omega})$. For any $\delta\theta \in \Theta$, we can form the function $g \, \delta\theta \cdot n$ which resides in $C^{0,1}(\hat{\Gamma})$ since $g \in C^{0,1}(\overline{D})$ and $n \in C^{0,1}(\hat{\Gamma}, \mathbb{R}^N)$ for a $C^{1,1}$ free boundary $\hat{\Gamma}$. Note that we can extend this to a function in $H^1_{0,\Gamma_\mathcal{D}}(\hat{\Omega})$. Hence, by setting $\delta u = -g \, \delta\theta \cdot n$, we obtain (4.11). ∎

5. Extension to nonsmooth free boundaries. In numerical computations the approximate free boundary is often piecewise smooth; i.e., $\hat{\Gamma}$ is Lipschitz continuous. In this case, the curvature term $\kappa = \operatorname{div}_\Gamma n$ is singular at singular points of the free boundary, and definition (4.4) of the dual problem does not apply. In this section, we extend the dual problem to Lipschitz free boundaries by introducing a generalization of the curvature term. Accordingly, we obtain goal-oriented error estimates for any approximation $(\hat{\Omega}, u^{\mathsf{h}}) \in \mathcal{O} \times H_h^1(\hat{\Omega})$ of our free-boundary problem. We note that similar generalizations of curvature terms have been studied in [10, 18, 26, 34].

5.1. Shape linearization at nonsmooth free boundaries. The singular contribution associated with κ appears in the shape derivative of the free-boundary problem weak form $\mathcal{N}$. Specifically, it originates from the shape linearization of $\mathcal{G}$. Therefore, a natural extension of this term can be obtained by extending this linearization to Lipschitz free boundaries. To derive this extension, we shall consider particular perturbation-vector fields $\delta\theta \in \Theta$.

Recall from the structure theorem, Theorem 3.1, that for sufficiently smooth boundaries, the significant perturbations are nonzero in the normal direction, i.e., $\delta\theta \cdot n \neq 0$. For Lipschitz domains $\hat{\Omega}$, a similar role shall be played by perturbations in a smoothened normal direction $m = m(\hat{\Gamma})$. This smoothened normal m is a bounded Lipschitz continuous vector field which is extendable onto D, i.e., $m \in C^{0,1}(\overline{D}, \mathbb{R}^N)$. Furthermore, we normalize m according to

$$m \cdot n = 1 \qquad \text{a.e. on } \hat{\Gamma}\,. \tag{5.1}$$

An example of m in two dimensions is illustrated in Figure 3. For the existence of m, see [20, p. 40] and [39], for example. We next define a particular perturbation in the m-direction as $\delta\theta = \delta\varrho\, m$. Here, $\delta\varrho$ is a scalar Lipschitz continuous function that vanishes on $\Gamma_{\mathcal{D}}$. The corresponding space for perturbations in the m-direction shall be denoted by $\Theta(m)$ and is defined as

$$\Theta(m) := \left\{ \delta\theta = \delta\varrho\, m \;\forall \delta\varrho \in C^{0,1}(\overline{D}) : \delta\varrho = 0 \text{ on } \Gamma_{\mathcal{D}} \right\}.$$

Note that these perturbations are admissible in the sense that $\Theta(m) \subset \Theta$.

We now turn to the shape linearization of $\Omega \mapsto \mathcal{G}(\Omega; v)$ for perturbations $\delta\varrho\, m$. Since the free boundary is nonsmooth, we apply Proposition 3.4 and obtain

$$\mathcal{G}'(\hat{\Omega}; v)(\delta\varrho\, m) = \left\langle g\, \partial_n v, \delta\varrho \right\rangle_{\hat{\Gamma}} + \int_{\hat{\Gamma}} \left(\partial_n g\, v\, \delta\varrho + \operatorname{div}_\Gamma(g\, v\, \delta\varrho\, m) \right), \tag{5.2}$$

where we invoked the normalization (5.1) two times. Comparing this result with the shape derivative of $\mathcal{G}$ in section 4.1, we observe that the curvature contribution has

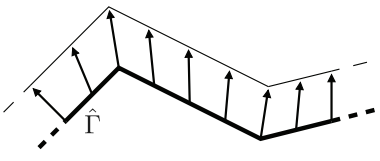

FIG. 3. *Illustration of a Lipschitz continuous m-vector field at the free boundary* $\hat{\Gamma}$. *The part of m that is orthogonal to* $\hat{\Gamma}$ *is equal to the normal n, that is,* $m \cdot n = 1$ *a.e. on* $\hat{\Gamma}$.

been replaced with a tangential divergence term. A suitable space for v in (5.2) is provided by the intersection $H^1_{0,\Gamma_\mathcal{D}}(\Delta;D)\cap \check{H}^1_{0,\Gamma_\mathcal{D}}(\hat{\Omega})$, where

$$\check{H}^1_{0,\Gamma_\mathcal{D}}(\hat{\Omega}) := \left\{ v\in H^1_{0,\Gamma_\mathcal{D}}(\hat{\Omega}) \middle|\ \textstyle\int_{\check{x}} |v|^2 \,\mathrm{d}\check{x} < \infty \ \forall \text{ singular points } \check{x}\subset\hat{\Gamma} \right\}.^3$$

The space $\check{H}^1_{0,\Gamma_\mathcal{D}}(\hat{\Omega})$ accounts for the boundedness of the tangential divergence term in (5.2). As this is not immediately clear, we show this in Appendix A, section A.1. We can now present an extension of Proposition 4.1 which holds for nonsmooth free boundaries. This result follows easily from the preceding developments.

PROPOSITION 5.1 (shape derivative of free-boundary problem). *Let $\hat{\Omega}\in\mathcal{O}$. For any $u^\mathsf{h}\in H^1_h(\hat{\Omega})\subset H^1(D)$ and $v\in H^1_{0,\Gamma_\mathcal{D}}(\Delta;D)\cap\check{H}^1_{0,\Gamma_\mathcal{D}}(\hat{\Omega})$, the shape functional $\Omega\mapsto\mathcal{N}((\Omega,u^\mathsf{h});v)$ is shape differentiable at $\hat{\Omega}$ with respect to $\Theta(m)$. Its shape derivative is given by*

$$\boxed{\begin{aligned}&\left\langle \partial_\Omega \mathcal{N}\big((\hat{\Omega},u^\mathsf{h});v\big),\delta\varrho\, m\right\rangle = \\ &\qquad -\left\langle g\,\partial_n v\,,\,\delta\varrho\right\rangle_{\hat{\Gamma}} - \int_{\hat{\Gamma}} \Big(\big(f+\partial_n g\big)\, v\,\delta\varrho + \mathrm{div}_\Gamma(g\,v\,\delta\varrho\, m)\Big)\,.\end{aligned}} \tag{5.3}$$

As a side remark, we note that for smooth ($C^{1,1}$) free boundaries, the results reduce to those of section 4.1. In fact, in the smooth case, $m=n$ is Lipschitz continuous, and we have $\check{H}^1_{0,\Gamma_\mathcal{D}}(\hat{\Omega}) = H^1_{0,\Gamma_\mathcal{D}}(\hat{\Omega})$. Furthermore, (5.3) reduces to (4.2b) since

$$\mathrm{div}_\Gamma(g\,v\,\delta\varrho\, n) = g\,v\,\delta\varrho\ \mathrm{div}_\Gamma\, n + \nabla_\Gamma(g\,v\,\delta\varrho)\cdot n = \kappa\, g\, v\,\delta\varrho\,,$$

and $\delta\varrho = \delta\theta\cdot n$.

5.2. Dual problem and goal-error estimate. Based on the extension of the linearization to Lipschitz domains $\hat{\Omega}$, we can introduce an analogous extension of the dual problem in (4.4). The extended dual problem relies on the smoothened normal field m introduced previously. Let z be the solution of the following variational problem:

$$\boxed{\begin{aligned}&\text{Find } z\in\check{H}^1_{0,\Gamma_\mathcal{D}}(\hat{\Omega}):\\ &\qquad \int_{\hat{\Omega}} \nabla\delta u\cdot\nabla z + \int_{\hat{\Gamma}} \left(\frac{1}{g}(f+\partial_n g)\, z\,\delta u + \mathrm{div}_\Gamma(z\,\delta u\, m)\right)\\ &\qquad\qquad = \int_{\hat{\Omega}} q^{\mathrm{ave}}\,\delta u - \int_{\hat{\Gamma}} \frac{1}{g}(q^{\mathrm{ave}}+q^{\mathrm{elev}})\,\delta u \qquad \forall \delta u\in\check{H}^1_{0,\Gamma_\mathcal{D}}(\hat{\Omega})\,.\end{aligned}} \tag{5.4}$$

The existence of unique solutions to (5.4) can be established based on a coercivity estimate under similar assumptions on the data as in section 4.3. As the derivation of this estimate is rather involved, we have deferred it to section A.2.

Analogous to the smooth case in Theorem 4.2, the dual problem in (5.4) provides a solution that is consistent with the linearization of $\mathcal{N}$ and $\mathcal{Q}$. The allowed domain perturbations in the linearization are, however, in the m-direction only. We summarize this dual consistency in the following theorem, whose proof is delayed to the end of this section.

[3] In two dimensions $\check{x}$ consists of zero-dimensional singular points $\check{x}_i\in\hat{\Gamma}$ and $\int_{\check{x}}|v|^2\,\mathrm{d}\check{x} = \sum_i |v(\check{x}_i)|^2$. In N dimensions $\check{x}$ is the $(N-2)$-dimensional subset of $\hat{\Gamma}$, where κ is singular.

THEOREM 5.2 (dual consistency). *Given an approximation* $(\hat{\Omega}, u^{\mathsf{h}}) \in \mathcal{O} \times H_h^1(\hat{\Omega})$ *of the solution* $(\Omega, u) \in \mathcal{O} \times H_h^1(\Omega)$ *of the free-boundary problem* (2.1)*, the solution* $z \in \check{H}^1_{0,\Gamma_{\mathcal{D}}}(\hat{\Omega}) \subset H^1(D)$ *of dual problem* (5.4) *satisfies*

$$\mathcal{N}'\big((\hat{\Omega}, u^{\mathsf{h}}); z\big)(\delta\theta, \delta u) = \mathcal{Q}'\big(\hat{\Omega}, u^{\mathsf{h}}\big)(\delta\theta, \delta u)$$

$\forall\ (\delta\theta, \delta u) \in \Theta(m) \times H^1_{0,\Gamma_{\mathcal{D}}}(D)$.

We immediately obtain a goal-oriented error estimate by the same arguments as in section 4.3. As the allowed domain perturbations are in the m-direction only, we first need to introduce a domain difference between Ω and $\hat{\Omega}$ along m. For this, let $e_\Omega(m) \in \Theta(m)$ such that $\Omega = T_{e_\Omega(m)}(\hat{\Omega})$.

PROPOSITION 5.3 (goal-error estimate). *Under the conditions of Theorem* 5.2*, let* $z \in \check{H}^1_{0,\Gamma_{\mathcal{D}}}(\hat{\Omega})$ *be the solution of dual problem* (4.4)*. It holds that*

$$\boxed{\mathcal{E}_{\mathcal{Q}} := \mathcal{Q}(\Omega, u) - \mathcal{Q}(\hat{\Omega}, u^{\mathsf{h}}) = \mathcal{R}\big((\hat{\Omega}, u^{\mathsf{h}}); z\big) + R\,,} \tag{5.5}$$

where the remainder R *is* $o(\|e_\Omega(m)\|, \|e_u\|)$.

Proof. The proof of this proposition follows by the same arguments as in the proof of Proposition 4.3. ∎

The dual problem in (5.4) is an extension of the dual problem in (4.4) in the sense that for smooth free boundaries, (5.4) reduces to (4.4). This can be verified by recalling that in this case $m = n$ and $\check{H}^1_{0,\Gamma_{\mathcal{D}}}(\hat{\Omega}) = H^1_{0,\Gamma_{\mathcal{D}}}(\hat{\Omega})$. Furthermore, we have

$$\operatorname{div}_\Gamma(z\,\delta u\, m) = z\,\delta u\, \operatorname{div}_\Gamma n + \nabla_\Gamma(z\,\delta u)\cdot n = \kappa\, z\,\delta u\,.$$

Proof of Theorem 5.2. As in the proof of Theorem 4.2, we consider the u- and Ω-linearized equations separately. The satisfaction of

$$\big\langle \partial_u \mathcal{N}\big((\hat{\Omega}, u^{\mathsf{h}}); z\big), \delta u\big\rangle = \big\langle \partial_u \mathcal{Q}(\hat{\Omega}, u^{\mathsf{h}}), \delta u\big\rangle \qquad \forall \delta u \in H^1_{0,\Gamma_{\mathcal{D}}}(D)$$

follows from the same variational arguments as in the proof of Theorem 4.2. As a result, we obtain $-\Delta z = q^{\text{ave}}$ in $\hat{\Omega}$, and thus, $z \in H^1_{0,\Gamma_{\mathcal{D}}}(\Delta; D) \cap \check{H}^1_{0,\Gamma_{\mathcal{D}}}(\hat{\Omega})$. We are left with showing that z satisfies the Ω-linearized equation defined by (5.3) and (4.3b):

$$-\big\langle g\,\partial_n z\,,\,\delta\varrho\big\rangle_{\hat{\Gamma}} - \int_{\hat{\Gamma}} \Big(\big(f + \partial_n g\big)\, z\,\delta\varrho + \operatorname{div}_\Gamma(g\, z\,\delta\varrho\, m)\Big) = \int_{\hat{\Gamma}} \big(q^{\text{ave}} + q^{\text{elev}}\big)\,\delta\varrho \tag{5.6}$$

$\forall\ \delta\varrho \in C^{0,1}(\overline{D})$ with $\delta\varrho = 0$ on $\Gamma_{\mathcal{D}}$. To show this, we integrate by parts the first integral in (5.4) to obtain

$$\big\langle \partial_n z, \delta u\big\rangle_{\hat{\Gamma}} + \int_{\hat{\Gamma}} \left(\frac{1}{g}(f + \partial_n g)\, z\,\delta u + \operatorname{div}_\Gamma(z\,\delta u\, m)\right) = -\int_{\hat{\Gamma}} \frac{1}{g}(q^{\text{ave}} + q^{\text{elev}})\,\delta u$$

$\forall\ \delta u \in H^1_{0,\Gamma_{\mathcal{D}}}(\hat{\Omega})$. Choosing $\delta u = -g\,\delta\varrho \in H^1_{0,\Gamma_{\mathcal{D}}}(\hat{\Omega})$, we obtain (5.6). ∎

6. Numerical experiments. To enable a comparison between the shape-linearization approach and the domain-map linearization of [42], we consider the same numerical experiments as in [42]. We demonstrate that the shape-linearization approach provides an elegant alternative to the domain-map linearization approach. First, we consider in section 6.1 the Bernoulli-type free-boundary problem in one dimension. The shape linearization of this one-dimensional problem is essentially equivalent to the so-called total linearization method used in [3] to obtain a Newton-type solution algorithm. In section 6.2, we consider the Bernoulli-type free-boundary problem in two dimensions. We demonstrate the effectivity of the dual-based error estimate on uniformly refined meshes and present an example of goal-oriented adaptive mesh refinement.

6.1. One-dimensional application. In the one-dimensional setting, the variable domain is the interval $\Omega = (0, \vartheta) \subset \mathbb{R}$. The Dirichlet boundary and free boundary are the points $\Gamma_{\mathcal{D}} = \{0\}$ and $\Gamma = \{\vartheta\}$, respectively. The approximate domain is given by $\hat{\Omega} = (0, \vartheta^{\mathsf{h}})$. It can be verified that the dual problem (4.4) reduces in the one-dimensional setting to: Find $z \in H^1_{0,\Gamma_{\mathcal{D}}}(\hat{\Omega})$:

$$\int_{\hat{\Omega}} \delta u_x \, z_x \, \mathrm{d}x + \left(\frac{1}{g}(f + g_x) \, z \, \delta u \right)(\vartheta^{\mathsf{h}}) = \int_{\hat{\Omega}} q^{\mathrm{ave}} \, \delta u \, \mathrm{d}x - \left(\frac{1}{g}(q^{\mathrm{ave}} + q^{\mathrm{elev}}) \, \delta u \right)(\vartheta^{\mathsf{h}})$$

$\forall \, \delta u \in H^1_{0,\Gamma_{\mathcal{D}}}(\hat{\Omega})$, where $(\cdot)_x = \mathrm{d}(\cdot)/\mathrm{d}x$ and $q^{\mathrm{elev}} \in \mathbb{R}$.[4]

6.1.1. Typical error estimate. We consider the data and goal functionals and the corresponding exact solution as indicated in Table 1. To show some typical error estimation results, consider the following approximation and corresponding goal values:

$$\left(\vartheta^{\mathsf{h}}, u^{\mathsf{h}}(x)\right) = \left(\frac{3}{2}, \frac{2}{3}x\right), \qquad \mathcal{Q}^{\mathrm{ave}}\left(\vartheta^{\mathsf{h}}; u^{\mathsf{h}}\right) = \frac{3}{4}, \qquad \mathcal{Q}^{\mathrm{elev}}\left(\vartheta^{\mathsf{h}}\right) = \frac{3}{2}.$$

TABLE 1
Specification of the data for the one-dimensional example.

$f(x)$	$g(x)$	$q^{\mathrm{ave}}(x)$	q^{elev}	ϑ	$u(x)$	$\mathcal{Q}^{\mathrm{ave}}(\vartheta; u)$	$\mathcal{Q}^{\mathrm{elev}}(\vartheta)$
$-\frac{1}{2}$	$x - 1$	1	1	2	$\frac{1}{4}x^2$	$\frac{2}{3}$	2

Figure 4 (left) shows a graphical illustration of the exact and approximate solutions. Furthermore, Figure 4 (right) shows the dual solutions for $\mathcal{Q}^{\mathrm{ave}}$ and $\mathcal{Q}^{\mathrm{elev}}$:

$$z^{\mathrm{ave}}(x) = \frac{1}{4}x - \frac{1}{2}x^2, \qquad z^{\mathrm{elev}}(x) = -\frac{4}{5}x.$$

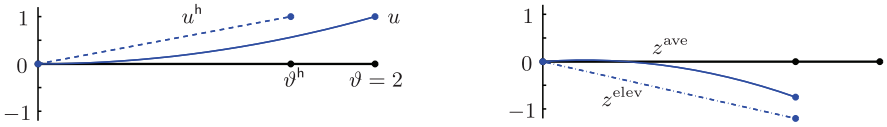

FIG. 4. *Exact solution* (ϑ, u) *and approximation* $(\vartheta^{\mathsf{h}}, u^{\mathsf{h}})$ *(left). Dual solutions* z^{ave} *and* z^{elev} *corresponding to goal functionals* $\mathcal{Q}^{\mathrm{ave}}$ *and* $\mathcal{Q}^{\mathrm{elev}}$*, respectively (right).*

The corresponding dual-based error estimate, $\mathrm{Est}_{\mathcal{Q}} := \mathcal{R}\big((\hat{\Omega}, u^{\mathsf{h}}); z\big) = \int_{\hat{\Omega}} f \, z \, \mathrm{d}x + (g \, z)(\vartheta^{\mathsf{h}}) - \int_{\hat{\Omega}} u^{\mathsf{h}}_x \, z_x \, \mathrm{d}x$, and the true goal error, $\mathcal{E}_{\mathcal{Q}}$, are as follows:

$$\mathrm{Est}_{\mathcal{Q}^{\mathrm{ave}}} = \frac{17}{64}, \qquad \mathrm{Est}_{\mathcal{Q}^{\mathrm{elev}}} = \frac{13}{20},$$
$$\mathcal{E}_{\mathcal{Q}^{\mathrm{ave}}} = -\frac{1}{12}, \qquad \mathcal{E}_{\mathcal{Q}^{\mathrm{elev}}} = \frac{1}{2}.$$

The difference in the error estimate and the true error is caused by linearization. Let us note that both the dual solutions and error estimates are slightly different from the results obtained by means of the domain-map linearization approach of [42].

[4]Let us note that in the one-dimensional setting, the use of shape calculus is, of course, not necessary as one can use the Leibniz integral rule to differentiate under the integral sign.

6.1.2. Convergence of error estimates. In the following example, the data is again specified as in Table 1. We investigate the convergence of the dual-based error estimate for the following $\Delta\vartheta$-family of approximate solutions:[5]

$$\vartheta^{\mathsf{h}} = \vartheta + \Delta\vartheta \,, \tag{6.1a}$$

$$u^{\mathsf{h}}(x) = \begin{cases} u(x) & x \in [0,\vartheta] \,, \\ u(\vartheta) & x \in (\vartheta, \vartheta+\Delta\vartheta] \,. \end{cases} \tag{6.1b}$$

This family converges to the exact solution as $\Delta\vartheta \searrow 0$. Note that u^{h} is simply a constant extension of u on the approximate domain. Hence, if u is conceived of as a member of $H^1_{0,\Gamma_{\mathcal{D}}}(\hat{\Omega})$ by constant extension outside $[0,\vartheta]$, then $e_u = u - u^{\mathsf{h}} = 0$. From the perspective of the error representation (see Proposition 4.3), only the error $e_\Omega = \Delta\vartheta$ is then relevant.

Figure 5 (left) plots the actual error $\mathcal{E}_{\mathcal{Q}^{\mathrm{ave}}}$ and the dual-based estimate $\mathrm{Est}_{\mathcal{Q}^{\mathrm{ave}}}$ versus $\Delta\vartheta$ for the goal functional $\mathcal{Q}^{\mathrm{ave}}$. Furthermore, Figure 5 (right) plots the error in the estimate $|\mathcal{E}_{\mathcal{Q}^{\mathrm{ave}}} - \mathrm{Est}_{\mathcal{Q}^{\mathrm{ave}}}|$ versus the norm of the error:

$$\left\|(e^\vartheta, e^u)\right\|^2 = |\vartheta - \vartheta^{\mathsf{h}}|^2 + \|u_x - u^{\mathsf{h}}_x\|^2_{L^2(\hat{\Omega})} = |\Delta\vartheta|^2 \,.$$

Both parts of Figure 5 illustrate that the convergence of the estimate is indeed second-order, in accordance with the theory.

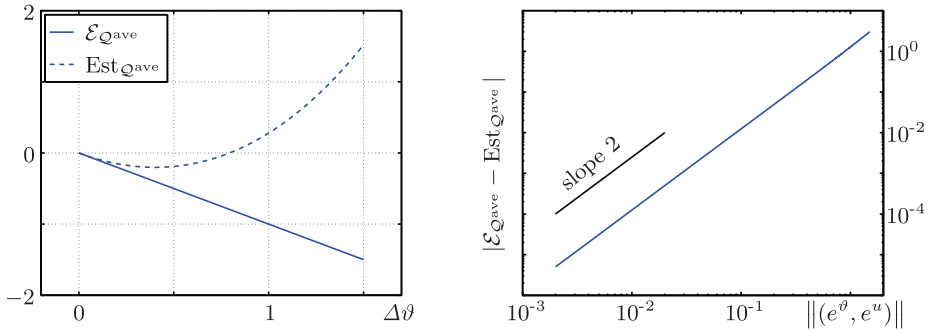

FIG. 5. *True goal error* $\mathcal{E}_{\mathcal{Q}^{\mathrm{ave}}}$ *and dual-based error estimate* $\mathrm{Est}_{\mathcal{Q}^{\mathrm{ave}}}$ *for the* $\Delta\vartheta$*-family of approximations* $(\vartheta^{\mathsf{h}}, u^{\mathsf{h}})$ *given in* (6.1a) *and* (6.1b) *(left). Convergence of the error in the error estimate with respect to the norm* $\|(e^\vartheta, e^u)\|$ *(right).*

6.2. Two-dimensional application. We now consider the two-dimensional case. We denote coordinates by $(x,y) \in \mathbb{R}^2$. We compute approximations of (2.2) by means of Galerkin's method. Hence, the approximate domain $\hat{\Omega} \in \mathcal{O}$ and corresponding approximate solution $u^{\mathsf{h}} \in V^{\mathsf{h}}_h(\hat{\Omega})$ satisfy

$$\int_{\hat{\Omega}} \nabla u^{\mathsf{h}} \cdot \nabla v = \int_{\hat{\Omega}} f\, v + \int_{\hat{\Gamma}} g\, v$$

$\forall\, v \in V^{\mathsf{h}}_{0,\Gamma_{\mathcal{D}}}(\hat{\Omega})$, where $V^{\mathsf{h}}_h(\hat{\Omega}) \subset H^1_h(\hat{\Omega})$ and $V^{\mathsf{h}}_{0,\Gamma_{\mathcal{D}}}(\hat{\Omega}) \subset H^1_{0,\Gamma_{\mathcal{D}}}(\hat{\Omega})$ denote standard finite element spaces consisting of piecewise-linear functions on triangles. Accordingly, the approximate free boundary is a piecewise-linear curve composed of the edges of

[5] To arrive at a convenient expression for the norm of the error, the family of approximations in (6.1) is slightly different from that in [42].

the adjacent elements. The nonlinear problem is solved using a fixed point iteration similar to the explicit Neumann scheme in [16], where we allow the vertices of the free boundary to move only vertically.

Since our approximate domains have piecewise-linear free boundaries, we have to use the dual problem (5.4). This dual problem is discretized on the same triangular mesh as the primal problem but with piecewise-quadratic functions (that vanish on $\Gamma_{\mathcal{D}}$). The tangential divergence term in (5.4) is implemented by means of identity (A.2); see Appendix A for more details.

6.2.1. Effectivity for the parabolic free-boundary test case. First, we reconsider the parabolic free-boundary test case introduced in [42]; see Figure 6 for the geometric layout. The data $\{f, g, h\}$ of the free-boundary problem is manufactured to yield the exact domain $\Omega = (0, 2) \times (0, 1 + \alpha_\Omega)$, with

$$\alpha_\Omega(x) = \frac{1}{2}\, x\,(2 - x)\ ,$$

and the corresponding solution

$$u(x, y) = \frac{y}{1 + \alpha_\Omega(x)} + \alpha_\Omega(x)\, \frac{y}{1 + \alpha_\Omega(x)} \left(1 - \frac{y}{1 + \alpha_\Omega(x)}\right)\ .$$

Our interest pertains to the average goal with $q^{\text{ave}} = 1$, which yields $Q^{\text{ave}}(\Omega; u) = 67/45 = 1.4888\ldots$ at the solution. In Figure 6, we depict the approximate dual solution z for the coarsest mesh and a very fine mesh. The convergence of the corresponding dual-based error estimates $\text{Est}_{\mathcal{Q}^{\text{ave}}} = \mathcal{R}((\hat{\Omega}, u^{\text{h}}); z)$ on uniformly refined meshes is reported in Table 2. The effectivity index $\text{Est}_{\mathcal{Q}^{\text{ave}}}/\mathcal{E}_{\mathcal{Q}^{\text{ave}}}$ approaches 1, demonstrating the consistency of the error estimate. The small deviation from 1 is conjecturally caused by weak singularities in the dual solution at the kinks in the approximate free boundary. To enable a comparison, Table 2 also presents the results obtained in [42] for the domain-map linearization approach. On coarse meshes, shape linearization yields a more accurate estimate than domain-map linearization. However, the results of both approaches are essentially identical.

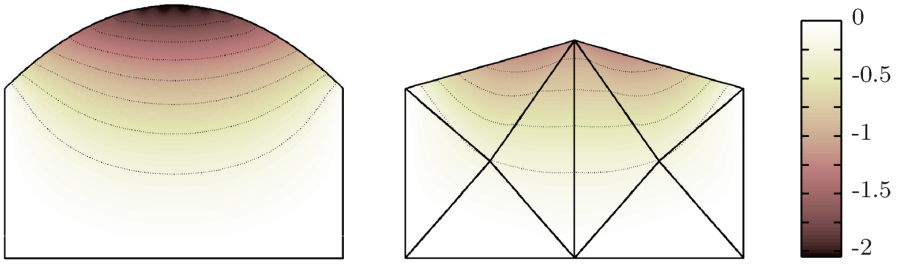

FIG. 6. *Test problem of section* 6.2.1. *The approximate dual solution (contour plot) associated with a very fine mesh (left) and the coarsest mesh (right).*

6.2.2. Goal-oriented adaptivity for free-surface flow over a bump. To investigate the applicability of the error estimate to drive adaptive mesh refinement, we regard the problem of free-surface flow over a bump of [42] with domain $\Omega = (0, 4) \times (y^b, 1 + \alpha_\Omega)$; see Figure 7 (top). The function y^b describes the bottom and has triangular bump at $1 < x < 2$. For the data, we take $f = 0$ and $g = 1$. Moreover,

TABLE 2
Convergence of the dual-based error estimate $\mathrm{Est}_{\mathcal{Q}^{\mathrm{ave}}}$ *under uniform mesh refinement for the shape-linearization approach and the domain-map linearization approach of* [42].

				Shape		Domain map	
Elements	DOFs	$\mathcal{Q}^{\mathrm{ave}}$	$\mathcal{E}_{\mathcal{Q}^{\mathrm{ave}}}$	$\mathrm{Est}_{\mathcal{Q}^{\mathrm{ave}}}$	Effect.	$\mathrm{Est}_{\mathcal{Q}^{\mathrm{ave}}}$	Effect.
8	8	1.1573	0.33163	0.32160	0.970	0.22131	0.667
16	15	1.3145	0.17440	0.16101	0.923	0.13852	0.794
32	23	1.3694	0.11947	0.12285	1.028	0.09994	0.836
64	45	1.4284	0.06045	0.06044	1.000	0.05499	0.910
128	77	1.4555	0.03339	0.03584	1.073	0.03055	0.915
256	153	1.4715	0.01740	0.01810	1.040	0.01676	0.963
512	281	1.4803	0.00860	0.00933	1.085	0.00808	0.940
1,024	561	1.4843	0.00458	0.00482	1.054	0.00450	0.984
2,048	1,073	1.4867	0.00217	0.00235	1.083	0.00205	0.947
4,096	2,145	1.4877	0.00117	0.00123	1.057	0.00115	0.991
8,192	4,193	1.4883	0.00054	0.00059	1.081	0.00051	0.949
16,384	8,385	1.4886	0.00029	0.00031	1.057	0.00029	0.993
∞	∞	1.4888	0				

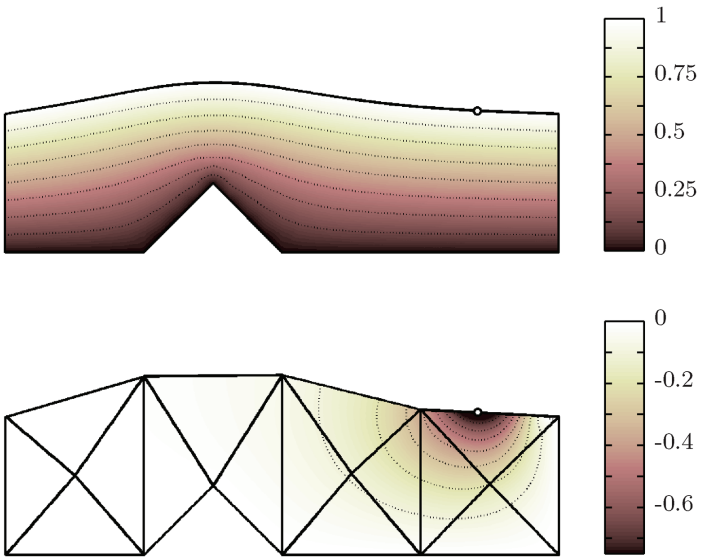

FIG. 7. *Test problem of section* 6.2.2. *The exact domain and solution (contour plot) (top) and the approximate domain and dual solution corresponding to the coarsest mesh (bottom). We have indicated the free-boundary elevation point of interest (at* $x_0 = 2 + \sqrt{2}$*).*

h is 0 at the bottom and increases linearly to 1 along the lateral boundaries of the domain. Our interest is the elevation of the free boundary at $x_0 = 2 + \sqrt{2}$. Figure 7 (bottom) displays the corresponding coarsest mesh dual solution. We construct element refinement indicators, apply a Dörfler-type marking, and refine using newest vertex bisection as in [42].

In Figure 8, we plot the error estimate and the "true" error versus the total number of degrees of freedom, which is denoted by n. The reference value $\mathcal{Q}^{\mathrm{elev}}(\theta) \approx 0.02271$ has been taken from [42]. The drop in the true error for the adaptive case for $\mathsf{n} > 1{,}000$ is caused by the nonnegligible error in the reference value. The adaptive refinement yields an optimal convergence rate of $\mathcal{O}(\mathsf{n}^{-1})$, while

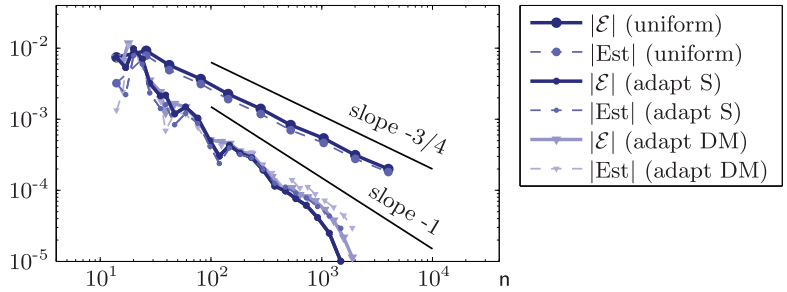

FIG. 8. *Convergence of the "true" error* $\mathcal{E} = \mathcal{E}_{\mathcal{Q}^{\text{elev}}}$ *and error estimate* $\text{Est} = \text{Est}_{\mathcal{Q}^{\text{elev}}}$ *under uniform mesh refinement, adaptive mesh refinement using shape linearization (adapt S), and adaptive mesh refinement using domain-map linearization* [42] *(adapt DM) versus the total number of degrees of freedom* n.

a suboptimal convergence rate of $\mathcal{O}(\mathsf{n}^{-3/4})$ is obtained for uniform refinement. Figure 8 also shows that the convergence behavior of adaptive refinement with shape linearization and with domain-map linearization is similar.

Figure 9 (left) presents several adaptively refined meshes obtained by shape linearization. The different refinements at the three bump corners as well as the local refinement near the elevation point of interest are noteworthy. For comparison, Figure 9 (right) recalls from [42] the sequence of adaptively refined meshes obtained with domain-map linearization. The meshes in Figure 9 (left) have been selected in such a manner that they have similar numbers of elements. Note, however, that owing to our marking strategy, the corresponding iteration number can be distinct. It is to be noted that the domain-map linearization approach yields significantly more refinement near the free boundary. This is in line with the analysis in section 4.3, which conveys that the difference between the two approaches consists of a residual-type boundary term. However, although the refinements are different, both approaches give similar and optimal convergence behavior; see Figure 8.

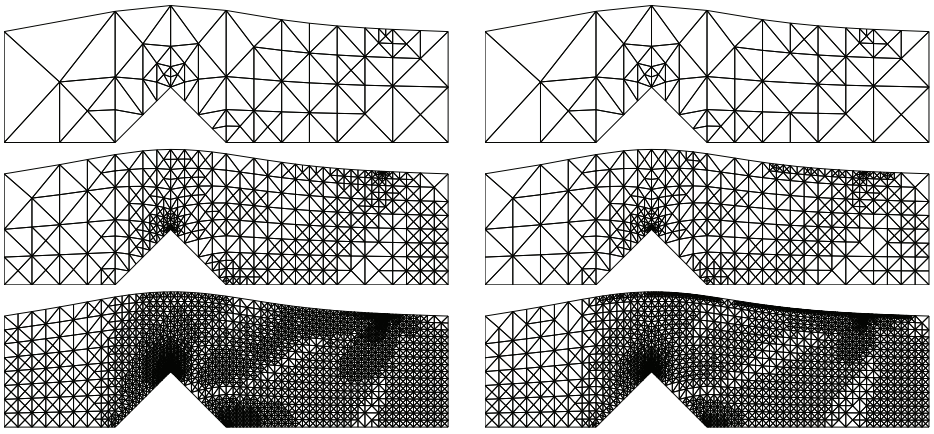

FIG. 9. *Adaptively refined meshes, controlling the error in the free-boundary elevation at* $x_0 = 2 + \sqrt{2}$*, obtained with shape linearization (left) after* 10, 18, *and* 26 *iterations (*120, 848, *and* 5,408 *elements, respectively) and with domain-map linearization* [42] *(right) after* 10, 18, *and* 29 *iterations (*120, 793, *and* 5,447 *elements, respectively).*

7. Concluding remarks. On the basis of a Bernoulli-type free-boundary problem, we presented a shape-linearization approach to goal-oriented error estimation for free-boundary problems. We showed that the associated very weak form and goal functional of interest can be formulated as a function of the unknown domain. The domain dependence was linearized using techniques from shape calculus. We extracted from the linear (adjoint) equation an appropriate dual problem by means of a consistent reformulation. This dual problem corresponds to a Poisson problem with a Robin-type boundary condition involving the curvature. Moreover, we derived a generalization of the dual problem for nonsmooth free boundaries which includes a natural extension of the curvature term. To demonstrate the effectivity of the dual-based error estimate and its usefulness in goal-oriented adaptive mesh refinement, we presented numerical experiments in one and two dimensions.

The shape-linearization approach provides an attractive alternative to the domain-map linearization approach in [42], as it avoids the nonstandard and nonlocal interior and boundary terms of the latter. We showed that the essential difference between the two approaches is that the dual problem in [42] contains a nonlocal residual-type boundary term. At the solution of the free-boundary problem, this residual-type term vanishes and both dual problems are equivalent. A comparison of the numerical results obtained by shape linearization with the results obtained in [42] by domain-map linearization revealed no essential differences.

Various extensions of our model problem can be envisaged. For example, we considered constant Dirichlet data at the free boundary and conforming u^{h} in the sense that $u^{\mathsf{h}} = h = 1$ on $\hat{\Gamma}$. This is convenient as the shape linearization of the associated combined term $-\mathcal{B}(\Omega; u^{\mathsf{h}}, v) + \mathcal{H}(\Omega; v)$ vanishes; see section 4.1. However, nonconstant $h|_\Gamma$ and $u^{\mathsf{h}} \neq h$ on $\hat{\Gamma}$ can be included if the associated terms are shape linearized accordingly. As a result, additional terms involving the Laplace–Beltrami operator appear in the dual $\hat{\Gamma}$-boundary condition. However, this requires additional regularity on the dual solution.

Another extension concerns more complicated free-boundary problems. In [40, 41], for example, the presented domain-map and shape-linearization approaches are considered in the context of a fluid-structure-interaction problem.

Instead of deriving linearized adjoints, the present shape-linearization approach can also be used to obtain Newton-based iteration algorithms for free-boundary problems; cf. [26–28]. The use of shape calculus appears to provide a convenient rigorous setting compared to formal asymptotic developments as in [2, 16]. The proposed extension to nonsmooth free boundaries in section 5, however, has to our knowledge not been considered before in this context. This extension provides a natural generalization of curvatures to nonsmooth free boundaries, obviating heuristic curvature reconstruction.

Appendix A. Additional analysis of the dual problem of section 5. In this section we provide auxiliary results concerning the dual problem in (5.4). We consider the two-dimensional case; the extension to three (and higher) dimensions follows similarly.

A.1. Boundedness of the tangential divergence term. Here, we verify the boundedness of the functional $v \mapsto \mathcal{K}(v) := \int_{\hat{\Gamma}} \operatorname{div}_\Gamma(g\, v\, \delta\rho\, m)$ (see (5.2)) on $\check{H}^1_{0,\Gamma_{\mathcal{D}}}(\hat{\Omega})$. Observe that, in two dimensions, any $v \in \check{H}^1_{0,\Gamma_{\mathcal{D}}}(\hat{\Omega})$ satisfies the constraint $|v(\check{x}_i)|^2 < \infty$ for singular points $\check{x}_i \in \hat{\Gamma}$, $i = 0, 1, \ldots$. The integral in $\mathcal{K}(v)$ can be integrated by parts (piecewise) resulting in contributions at these singular points. This requires

the tangential Stokes theorem on piecewise smooth boundaries. Let us denote the boundary segments between $\check{x}_i$ and $\check{x}_{i+1}$ by $\hat{\Gamma}_{i+1}$; see Figure 10. Note that $\hat{\Gamma} = \operatorname{int} \overline{\cup_i \hat{\Gamma}_i}$. Furthermore, let $\check{\tau}_i$ denote the vector at $\check{x}_i$ composed of the two unit tangent vectors $\tau|_{\hat{\Gamma}_i}$ and $\tau|_{\hat{\Gamma}_{i+1}}$ at $\check{x}_i$ outward with respect to their segment, i.e.,

$$\check{\tau}_i := \tau\big|_{\hat{\Gamma}_{i+1}}(\check{x}_i) + \tau\big|_{\hat{\Gamma}_i}(\check{x}_i) \, .$$

For points $\check{x}_i$ at the boundary of $\hat{\Gamma}$, $\check{\tau}_i$ is equal to the outward tangent vector. Then the following tangential identity holds:

$$\int_{\hat{\Gamma}} \operatorname{div}_\Gamma \theta = \sum_i \theta(\check{x}_i) \cdot \check{\tau}_i + \sum_i \int_{\hat{\Gamma}_i} \kappa \, \theta \cdot n \tag{A.1}$$

for suitable $\theta : \hat{\Gamma} \to \mathbb{R}^2$; see [36, p. 150] or [9], for example. Applying this to the integral in $\mathcal{K}(v)$, we have

$$\mathcal{K}(v) = \int_{\hat{\Gamma}} \operatorname{div}_\Gamma(g \, v \, \delta\rho \, m) = \sum_i (g \, v \, \delta\rho)(\check{x}_i) \, m(\check{x}_i) \cdot \check{\tau}_i + \sum_i \int_{\hat{\Gamma}_i} \kappa \, g \, v \, \delta\rho \, ,$$

where we used $m \cdot n = 1$ on $\hat{\Gamma}_i$. This leads to the bound

$$\mathcal{K}(v) \leq \sum_i |g(\check{x}_i) \, \delta\rho(\check{x}_i)| \, |v(\check{x}_i)| \, |m(\check{x}_i) \cdot \check{\tau}_i| + \sum_i \Big| \int_{\hat{\Gamma}_i} \kappa \, g \, v \, \delta\rho \, \Big| \, .$$

It now follows that $\mathcal{K}$ is bounded on $\check{H}^1_{0,\Gamma_{\mathcal{D}}}(\hat{\Omega})$ because the first sum is bounded in view of $|v(\check{x}_i)|^2 < \infty$ and the second sum is bounded for $v \in H^1(\hat{\Omega})$.

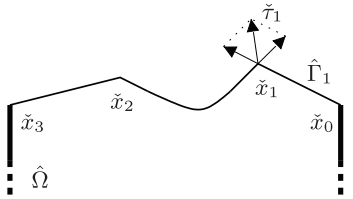

FIG. 10. *Illustration of the singular points $\check{x}_i$, a boundary segment $\hat{\Gamma}_i$, and a vector $\check{\tau}_i$ (composed of the two unit tangent vectors) for a domain $\hat{\Omega}$ with a piecewise smooth free boundary $\hat{\Gamma}$.*

A.2. Well posedness by coercivity. On account of the Lax–Milgram theorem, well posedness of the dual problem (5.4) follows from coercivity with respect to $\check{H}^1_{0,\Gamma_{\mathcal{D}}}(\hat{\Omega})$ of the corresponding bilinear form [6]

$$\mathcal{B}(\delta u, z) := \int_{\hat{\Omega}} \nabla \delta u \cdot \nabla z + \int_{\hat{\Gamma}} \left(\frac{1}{g}(f + \partial_n g) \, z \, \delta u + \operatorname{div}_\Gamma(z \, \delta u \, m) \right) \, .$$

Using the tangential identity (A.1), we can rewrite the tangential divergence term as

$$\int_{\hat{\Gamma}} \operatorname{div}_\Gamma(z \, \delta u \, m) = \sum_i \big(z \, \delta u\big)(\check{x}_i) \, m(\check{x}_i) \cdot \check{\tau}_i + \sum_i \int_{\hat{\Gamma}_i} \kappa \, z \, \delta u \, . \tag{A.2}$$

[6] The necessary continuity of the linear form is straightforward, and continuity of the bilinear form follows using similar arguments as in section A.1 for the tangential divergence term.

It follows that

$$\mathcal{B}(z,z) = \int_{\hat\Omega} |\nabla z|^2 + \sum_i \int_{\hat\Gamma_i} \frac{1}{g}(f + \partial_n g + \kappa\, g)\, z^2 + \sum_i z^2(\check{x}_i)\, m(\check{x}_i)\cdot \check{\tau}_i \ .$$

In view of the results in section A.1, a suitable norm on $\check{H}^1_{0,\Gamma_{\mathcal{D}}}(\hat\Omega)$ is given by

$$\|z\|^2_{\check{H}^1_{0,\Gamma_{\mathcal{D}}}(\hat\Omega)} := \int_{\hat\Omega} |\nabla z|^2 + \sum_i |z(\check{x}_i)|^2 \ .$$

It is now clear how to obtain sufficient conditions to ensure that $\mathcal{B}$ is coercive on $\check{H}^1_{0,\Gamma_{\mathcal{D}}}(\hat\Omega)$. If the domain is convex at the singular points in the sense that $m(\check{x}_i)\cdot\check{\tau}_i \geq C > 0\ \forall\ i$, and if, furthermore, $(f+\partial_n g)/g + \kappa \geq 0$ on $\hat\Gamma_i\ \forall\ i$, then

$$\mathcal{B}(z,z) \geq C\, \|z\|^2_{\check{H}^1_{0,\Gamma_{\mathcal{D}}}(\hat\Omega)} \qquad \forall z \in \check{H}^1_{0,\Gamma_{\mathcal{D}}}(\hat\Omega) \ .$$

Hence, under these conditions, the dual problem (5.4) has a unique solution in $\check{H}^1_{0,\Gamma_{\mathcal{D}}}(\hat\Omega)$.

We remark that similar conditions on the data are given in [12, 13]. Related boundary value problems with so-called oblique boundary conditions involving tangential derivatives are analyzed in [20, p. 167] and [4, p. 398].

Appendix B. Proof of Proposition 3.3. The proof follows by showing that the limit $t \to 0$ of a suitable bound on the difference quotient $(\mathcal{J}(\Omega_t) - \mathcal{J}(\Omega))/t$ vanishes. First, we note that the difference in $\mathcal{J}$ can be written as

$$\mathcal{J}(\Omega_t) - \mathcal{J}(\Omega) = \int_{\Omega_t} \phi_1\, \phi_2 - \int_{\Omega} \phi_1\, \phi_2 = \int_{\Delta\Omega_t} \beta\, \phi_1\, \phi_2,$$

where $\Delta\Omega_t := (\Omega_t \cup \Omega)\backslash(\Omega_t \cap \Omega)$ is the t-dependent set consisting of the nonoverlapping parts of Ω_t and Ω; see Figure 11 for an illustration in two dimensions. Furthermore, β is a scalar function that is -1 for the Ω part and 1 for the Ω_t part. Applying the Cauchy–Schwartz inequality, we have

$$\big|\mathcal{J}(\Omega_t) - \mathcal{J}(\Omega)\big| \leq \|\phi_1\|_{L^2(\Delta\Omega_t)}\, \|\phi_2\|_{L^2(\Delta\Omega_t)} \leq \|\phi_1\|_{L^2(D)}\, \|\phi_2\|_{L^2(\Delta\Omega_t)} \ .$$

An upper bound to the t-dependence of the second norm follows from the following Poincaré inequality.

LEMMA B.1. *For all $\phi_2 \in H^1(D)$ with $\phi_2 = 0$ on Γ, it holds that*

$$\|\phi_2\|_{L^2(\Delta\Omega_t)} \leq C\, t\, \|\nabla\phi_2\|_{L^2(\Delta\Omega_t)}$$

for some constant C independent of t.

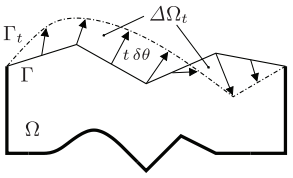

FIG. 11. *The perturbation of Ω by $t\,\delta\theta$ creates the t-dependent strip set $\Delta\Omega_t$.*

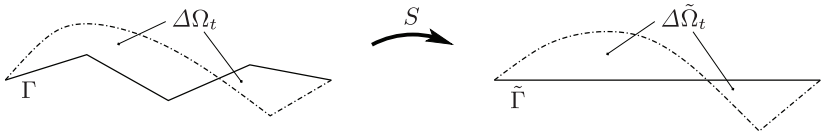

FIG. 12. *The boundary* Γ *of the strip set* $\Delta\Omega_t$ *is flattened under the Lipschitz continuous map* S.

The proof now follows straightforwardly:

$$\lim_{t\to 0} \big|\mathcal{J}(\Omega_t) - \mathcal{J}(\Omega)\big|/t \le \lim_{t\to 0} C\,\|\phi_1\|_{L^2(D)}\,\|\nabla\phi_2\|_{L^2(\Delta\Omega_t)} = 0\,.$$

Proof of Lemma B.1. Let $S : \overline{D} \to \overline{D}$ denote a bounded Lipschitz continuous transformation that maps Γ to the flat surface $\tilde{\Gamma}$ and $\Delta\Omega_t$ to $\Delta\tilde{\Omega}_t$; see Figure 12. Define $\tilde{\phi}_2 := \phi_2 \circ S^{-1}$. Then $\tilde{\phi} \in H^1(D)$ with $\tilde{\phi} = 0$ on $\tilde{\Gamma}$ (see [20, p. 21] or [7, p. 406]). Note that the domain $\Delta\tilde{\Omega}_t$ is bounded by a t-dependent cartesian box. The following Poincaré inequality with a t-dependent Poincaré constant holds for such slender domains:

$$\|\tilde{\phi}_2\|_{L^2(\Delta\tilde{\Omega}_t)} \le C\,t\,\|\nabla\tilde{\phi}_2\|_{L^2(\Delta\tilde{\Omega}_t)}\,;$$

see [22], for example. Substituting $\tilde{\phi}_2 := \phi_2 \circ S^{-1}$ and transforming back to $\Delta\Omega_t$ yields

$$\left(\int_{\Delta\Omega_t} \phi_2^2\,\det \mathrm{D}S\right)^{1/2} \le C\,t\left(\int_{\Delta\Omega_t} |\mathrm{D}S^{-\mathsf{T}}\nabla\phi_2|^2\,\det \mathrm{D}S\right)^{1/2}.$$

Noting that $\det \mathrm{D}S$ and the components of $\mathrm{D}S^{-\mathsf{T}}$ are in $L^\infty(D)$, we finally obtain the Poincaré inequality (with a different constant C). ∎

Acknowledgments. This research was supported by the Dutch Technology Foundation STW, applied science division of NWO, and the Technology Program of the Ministry of Economic Affairs.

REFERENCES

[1] R. Becker and R. Rannacher, *An optimal control approach to a posteriori error estimation in finite element methods*, Acta Numer., 10 (2001), pp. 1–102.

[2] F. Bouchon, S. Clain, and R. Touzani, *A perturbation method for the numerical solution of the Bernoulli problem*, J. Comput. Math., 26 (2008), pp. 23–36.

[3] C. Cuvelier and R. M. S. M. Schulkes, *Some numerical methods for the computation of capillary free boundaries governed by the Navier–Stokes equations*, SIAM Rev., 32 (1990), pp. 355–423.

[4] R. Dautray and J.-L. Lions, *Mathematical Analysis and Numerical Methods for Science and Technology,* Vol. 2: *Functional and Variational Methods*, Springer, Berlin, 1988.

[5] M. C. Delfour and J.-P. Zolésio, *Structure of shape derivatives for nonsmooth domains*, J. Funct. Anal., 104 (1992), pp. 1–33.

[6] M. C. Delfour and J.-P. Zolésio, *Tangential differential equations for dynamical thin/shallow shells*, J. Differential Equations, 128 (1996), pp. 125–167.

[7] M. C. Delfour and J.-P. Zolésio, *Shapes and Geometries: Analysis, Differential Calculus, and Optimization*, SIAM Ser. Adv. Design and Control 4, Society for Industrial and Applied Mathematics, Philadelphia, 2001.

[8] M. C. Delfour and J.-P. Zolésio, *Tangential calculus and shape derivatives*, in Shape Optimization and Optimal Design: Proceedings of the IFIP Conference, Lect. Notes Pure Appl. Math. 216, J. Cagnol, M. P. Polis, and J.-P. Zolésio, eds., Marcel Dekker, New York, 2001, pp. 37–60.

[9] F. R. Desaint and J.-P. Zolésio, *Manifold derivative in the Laplace-Beltrami equation*, J. Funct. Anal., 151 (1997), pp. 234–269.
[10] W. Dettmer and D. Perić, *A computational framework for free surface fluid flows accounting for surface tension*, Comput. Methods Appl. Mech. Engrg., 195 (2006), pp. 3038–3071.
[11] R. Djellouli, C. Farhat, J. Mandel, and P. Vaněk, *Continuous Fréchet differentiability with respect to a Lipschitz domain and a stability estimate for direct acoustic scattering problem*, IMA J. Appl. Math., 63 (1999), pp. 51–69.
[12] K. Eppler and H. Harbrecht, *Efficient treatment of stationary free boundary problems*, Appl. Numer. Math., 56 (2006), pp. 1326–1339.
[13] K. Eppler, H. Harbrecht, and R. Schneider, *On convergence in elliptic shape optimization*, SIAM J. Control Optim., 46 (2007), pp. 61–83.
[14] L. C. Evans and R. F. Gariepy, *Measure Theory and Fine Properties of Functions*, Stud. Adv. Math. 5, Chapman & Hall/CRC, Boca Raton, FL, 1992.
[15] J. Ferchichi and J.-P. Zolésio, *Shape sensitivity for the Laplace-Beltrami operator with singularities*, J. Differential Equations, 196 (2004), pp. 340–384.
[16] M. Flucher and M. Rumpf, *Bernoulli's free-boundary problem, qualitative theory and numerical approximation*, J. Reine Angew. Math., 486 (1997), pp. 165–204.
[17] G. Fremiot and J. Sokołowski, *The structure theorem for the Eulerian derivative of shape functionals defined in domains with cracks*, Sib. Math. J., 41 (2000), pp. 974–993. (Translation of Sibirsk. Mat. Zh., 41 (2000), pp. 1183-1203.)
[18] J.-F. Gerbeau and T. Lelièvre, *Generalized Navier boundary condition and geometric conservation law for surface tension*, Comput. Methods Appl. Mech. Engrg., 198 (2009), pp. 644–656.
[19] M. B. Giles and E. Süli, *Adjoint methods for PDEs: A posteriori error analysis and post-processing by duality*, Acta Numer., 11 (2002), pp. 145–236.
[20] P. Grisvard, *Elliptic Problems in Nonsmooth Domains*, Monogr. Stud. Math. 24, Pitman Publishing, London, 1985.
[21] J. S. Hadamard, *Mémoire sur le problème d'analyse relatif à l'équilibre des plaques élastiques encastrées*, in Œuvres de Jacques Hadamard, C.N.R.S. Editions, Paris, 1968, pp. 515–641. Originally published in Mém. Sav. Étrang., 33, 1907.
[22] I. Harari and T. J. R. Hughes, *What are C and h?: Inequalities for the analysis and design of finite element methods*, Comput. Methods Appl. Mech. Engrg., 97 (1992), pp. 157–192.
[23] J. Haslinger and P. Neittaanmäki, *Finite Element Approximation for Optimal Shape, Material and Topology Design*, 2nd ed., Wiley, New York, 1996.
[24] K. Ito, K. Kunisch, and G. H. Peichl, *Variational approach to shape derivatives for a class of Bernoulli problems*, J. Math. Anal. Appl., 314 (2006), pp. 126–149.
[25] K. Ito, K. Kunisch, and G. H. Peichl, *Variational approach to shape derivatives*, ESAIM Control Optim. Calc. Var., 14 (2008), pp. 517–539.
[26] K. T. Kärkkäinen, *Shape Sensitivity Analysis for Numerical Solution of Free Boundary Problems*, Ph.D. thesis, University of Jyväskylä, Jyväskylä, Finland, Jyväskylä Studies in Computing 58, 2005.
[27] K. T. Kärkkäinen and T. Tiihonen, *Free surfaces: Shape sensitivity analysis and numerical methods*, Internat. J. Numer. Methods Engrg., 44 (1999), pp. 1079–1098.
[28] K. T. Kärkkäinen and T. Tiihonen, *Shape calculus and free boundary problems*, in Proceedings of the European Congress on Computational Methods in Applied Sciences and Engineering, ECCOMAS 2004, P. Neittaanmäki, T. Rossi, S. Korotov, E. Oñate, J. Périaux, and D. Knörzer, eds., Jyväskylä, Finland, 2004.
[29] A. Laurain, *Structure of shape derivatives in non-smooth domains and applications*, Adv. Math. Sci. Appl., 15 (2005), pp. 199–226.
[30] G. Mejak, *Numerical solution of Bernoulli-type free boundary value problems by variable domain method*, Internat. J. Numer. Method Engrg., 37 (1994), pp. 4219–4245.
[31] A. Novruzi and M. Pierre, *Structure of shape derivatives*, J. Evol. Equ., 2 (2002), pp. 365–382.
[32] O. Pironneau, *Optimal Shape Design for Elliptic Systems*, Springer Ser. Comput. Phys., Springer, Berlin, 1984.
[33] S. Prudhomme and J. T. Oden, *Computable error estimators and adaptive techniques for fluid flow problems*, in Error Estimation and Adaptive Discretization Methods in Computational Fluid Dynamics, Lect. Notes Comput. Sci. Eng. 25, T. J. Barth and H. Deconinck, eds., Springer, Berlin, 2003, pp. 207–268.
[34] P. H. Saksono and D. Perić, *On finite element modelling of surface tension. Variational formulation and applications – Part* I: *Quasistatic problems*, Comput. Mech., 38 (2006), pp. 265–281.

[35] J. Simon, *Differentiation with respect to the domain in boundary-value-problems*, Numer. Funct. Anal. Optim., 2 (1980), pp. 649–687.
[36] J. Sokołowski and J.-P. Zolésio, *Introduction to Shape Optimization: Shape Sensitivity Analysis*, Springer Ser. Comput. Math. 16, Springer, Berlin, 1992.
[37] E. Süli and P. Houston, *Adaptive finite element approximation of hyperbolic problems*, in Error Estimation and Adaptive Discretization Methods in Computational Fluid Dynamics, Lect. Notes Comput. Sci. Eng. 25, T. J. Barth and H. Deconinck, eds., Springer, Berlin, 2003, pp. 269–344.
[38] J. I. Toivanen, J. Haslinger, and R. A. E. Mäkinen, *Shape optimization of systems governed by Bernoulli free boundary problems*, Comput. Methods Appl. Mech. Engrg., 197 (2008), pp. 3802–3815.
[39] E. H. van Brummelen, *Mesh association by projection along smoothed-normal-vector fields: Association of closed manifolds*, Internat. J. Numer. Methods Engrg., 73 (2008), pp. 493–520.
[40] K. G. van der Zee, *Goal-Adaptive Discretization of Fluid–Structure Interaction*, Ph.D. thesis, Technische Universiteit Delft, Delft, The Netherlands, June 2009. Available online from http://repository.tudelft.nl.
[41] K. G. van der Zee, E. H. van Brummelen, I. Akkerman, and R. de Borst, *Goal-oriented error estimation and adaptivity for fluid–structure interaction using exact linearized adjoints*, Comput. Methods Appl. Mech. Engrg., submitted.
[42] K. G. van der Zee, E. H. van Brummelen, and R. de Borst, *Goal-oriented error estimation and adaptivity for free-boundary problems: The domain-map linearization approach*, SIAM J. Sci. Comput., 32 (2010), pp. 1064–1092.
[43] J.-P. Zolésio, *Introduction to shape optimization problems and free boundary problems*, in Shape Optimization and Free Boundaries, NATO ASI Ser. C: Math. Phys. Sci. 380, M. C. Delfour and G. Sabidussi, eds., Kluwer Academic Publishers, Dordrect, 1992, pp. 397–457.